NACA TN No. 1516

NATIONAL ADVISORY COMMITTEE FOR AERONAUTICS

TECHNICAL NOTE

No. 1516

A GENERALIZED THEORETICAL AND EXPERIMENTAL INVESTIGATION OF THE MOTIONS AND HYDRODYNAMIC LOADS EXPERIENCED BY V-BOTTOM SEAPLANES DURING STEP-LANDING IMPACTS

By Benjamin Milwitzky

Langley Memorial Aeronautical Laboratory
Langley Field, Va.

Washington
February 1948

NATIONAL ADVISORY COMMITTEE FOR AERONAUTICS

TECHNICAL NOTE NO. 1516

A GENERALIZED THEORETICAL AND EXPERIMENTAL INVESTIGATION OF THE MOTIONS AND HYDRODYNAMIC LOADS EXPERIENCED BY V-BOTTOM SEAPLANES DURING STEP-LANDING IMPACTS

By Benjamin Milwitzky

SUMMARY

A theoretical investigation is made of the motions and hydrodynamic loads experienced by V-bottom seaplanes during the course of a step-landing impact. In the analysis the primary flow about the immersed portion of a keeled float or hull is considered to occur in transverse flow planes and the virtual-mass concept is applied to calculate the reaction of the water to the motion of the seaplane. The entire immersion process is analyzed from the instant of initial contact until the seaplane rebounds from the water surface and the conditions required for impact similarity are discussed.

By treating the variables of motion and time as dimensionless quantities, it is further shown that the variation of these quantities is governed by a single parameter κ, called the approach parameter, which is a function of the trim and the initial flight-path angle only. Thus, for a given value of κ, the respective variations during an impact of the nondimensional displacements, velocities, and accelerations may each be represented by a single curve, regardless of what the seaplane properties, attitude, or initial velocity may be. The use of dimensionless coefficients, by thus taking into account such factors as dead rise, weight, trim angle, and velocity in accordance with the laws governing the variation of the motion with these quantities, permits reduction of all time histories for the same approach parameter to a common basis. As a result, the number of solutions required to cover the entire range of seaplane and flight parameters is greatly decreased. Furthermore, the presentation of both theoretical and experimental results is simplified and a basis is provided for the ready correlation of large quantities of test data obtained under diverse conditions.

Equations are presented from which the time histories of the motion and the hydrodynamic loads have been calculated for a wide range of conditions extending from impacts along shallow flight paths approaching planing to impacts where the resultant velocity is normal to the keel. Solutions are also presented for the state of motion and the time corresponding to the instants of maximum acceleration, maximum draft, and rebound from the water surface.

An investigation of the effects of chine immersion on the maximum acceleration indicates that, for conventional beam loadings and flight-path angles, the decrease in load resulting from immersion of the chines is either small or entirely negligible. For higher beam loadings, however, the analysis reveals that appreciable load reductions can be expected.

The results of the investigation are presented in the form of dimensionless charts which may be directly used to determine the water loads and the motions of the seaplane at any instant during an impact as well as at the particular instants of maximum acceleration, maximum draft, and rebound. Extensive experimental data, obtained in the Langley impact basin with floats of $22\frac{1}{2}^\circ$, 30°, and 40° angles of dead rise for a wide range of conditions, are presented in support of the theoretical results.

INTRODUCTION

In order to provide a more rational foundation upon which to base water loading requirements for the design of seaplanes, an investigation of available hydrodynamic impact theories was undertaken by the National Advisory Committee for Aeronautics. As a result of this study, a critical survey of previously published works in the field was presented in reference 1, which showed that the former treatments are of limited applicability since they are valid only for zero trim impacts for which the resultant velocity is normal to the keel. The more general equations obtained by taking into consideration the effects of trim and components of motion parallel to the keel permit the analysis of practical seaplane impacts for the entire range of initial conditions extending from impacts along shallow flight paths approaching the planing condition to impacts where the resultant motion is normal to the keel.

In the present paper an analysis is made of the motion and hydrodynamic loads experienced by a prismatic V-bottom seaplane during step-landing impacts. From the relationship between the instantaneous hydrodynamic force and the displacement, velocity, and acceleration of the seaplane, the differential equation of motion is written which relates these variables at all times during the impact. The entire immersion process thus specified is analyzed from the instant of initial contact until the seaplane rebounds from the water surface and a number of additional relationships are presented which further describe the motion during the course of the impact. Since certain events during the immersion are of particular interest, the state of motion of the seaplane and the time of occurrence are also investigated for the instants of maximum acceleration, maximum draft, and rebound from the water surface.

From the equations presented it is further shown that the motion and time characteristics of a step impact are completely determined by a single parameter which depends on the attitude of the seaplane and the flight-path angle at the instant of initial contact with the water surface. This parameter, which may be considered a criterion of impact similarity, permits the formation of nondimensional coefficients which greatly condense and simplify the presentation of the significant impact variables.

The theoretical results are compared with extensive experimental data obtained in the Langley impact basin with floats of $22\frac{1}{2}^\circ$, 30°, and 40° angles of dead rise for a wide range of weights, trim angles, velocities, and flight-path angles.

SYMBOLS

A	hydrodynamic aspect ratio
b	beam
c	wetted semiwidth of cross section
F	hydrodynamic force
g	acceleration due to gravity
h	momentum of fluid within flow plane
l	wetted keel length
m_w	two-dimensional virtual mass
n_{i_w}	impact load factor, measured normal to water surface $\left(-\frac{\ddot{y}}{g}\right)$
r	rise of disturbed surface above level water surface
s	distance from given flow plane to foremost immersed station along keel
t	time after contact
V	velocity of seaplane
W	weight of seaplane
x	distance parallel to water surface

y	draft of keel at step, normal to water surface
z	penetration of given station, normal to keel
β	angle of dead rise
γ	flight-path angle relative to water surface
ρ	mass density of water
τ	trim angle
$f(\beta)$	dead-rise variation
$\phi(A)$	aspect ratio (end flow) correction

Subscripts:

ch	conditions at instant of chine immersion
o	initial conditions
p	parallel to keel
r	resultant
s	conditions at step

Dimensionless Variables

Approach parameter

$$\kappa = \frac{\sin \tau}{\sin \gamma_o} \cos \left(\tau + \gamma_o\right)$$

Load-factor coefficient

$$C_l = \frac{n_{l_w} g}{\dot{y}_o^2} \left(\frac{W}{g} \left\{ \frac{6 \sin \tau \cos^2 \tau}{\left[f(\beta)\right]^2 \phi(A) \rho \pi} \right\} \right)^{1/3}$$

Draft coefficient

$$C_d = y\left(\frac{g}{W}\left\{\frac{[f(\beta)]^2\phi(A)\rho\pi}{6 \sin\tau \cos^2\tau}\right\}\right)^{1/3}$$

Draft coefficient at chine immersion

$$C_{d_{ch}} = c_{s_{ch}}\left\{\frac{g}{W}\left[\frac{\phi(A)\rho\pi}{6f(\beta) \tan\tau}\right]\right\}^{1/3}$$

Time coefficient

$$C_t = t\dot{y}_o\left(\frac{g}{W}\left\{\frac{[f(\beta)]^2\phi(A)\rho\pi}{6 \sin\tau \cos^2\tau}\right\}\right)^{1/3}$$

Vertical-velocity ratio

$$\frac{\dot{y}}{\dot{y}_o}$$

ANALYSIS

Basis of Theory

The analysis is based on the concept (reference 1) that the primary flow about an immersing slender shape, such as a keeled seaplane float or hull, occurs in transverse planes which may be considered fixed in space and oriented essentially perpendicular to the keel. Because of the absence of a satisfactory three-dimensional theory, it is necessary to treat the motion of the fluid in each plane as a two-dimensional phenomenon independent of the other flow planes. In order to account for the losses which exist in the three-dimensional case, the total force on the float at any instant, which is obtained by summing up the reactions of the fluid in the individual flow planes in contact with the float, is reduced by the application of an end flow (aspect ratio) type correction $\phi(A)$. The effects of buoyancy and viscosity, which in an impact are normally small in comparison with the inertia forces, are neglected.

The flow process within a particular flow plane begins when the keel of the float penetrates the water surface and enters that plane. At all times thereafter, the momentum imparted to the water in the plane is determined solely by the growth of the float cross-sectional shape intersected by the plane and may be expressed as the product of the virtual mass associated with the immersed cross section and the velocity of penetration into the plane. In the case of a prismatic float, the component of motion parallel to the keel, which governs the number of flow planes encountered and thus the distribution of momentum between the water directly beneath the float and the downwash behind the step, has no effect on the momentum content of the fluid within the planes still in contact with the float. After the step has passed through a given flow plane, however, the intersected cross section ceases to exist and the plane becomes part of the downwash where it remains thereafter, independent of the subsequent progress of the impact.

The instantaneous reaction of the fluid contained in a given flow plane is determined by the rate at which momentum is imparted to the fluid within the plane. For a prismatic float, therefore, the force contributed by a particular flow plane is independent of the component of velocity parallel to the keel and is governed solely by the shape of the intersected cross section and the components of velocity and acceleration normal to the keel.

Although the component of velocity parallel to the keel has no effect on the state of motion of the fluid within the individual flow planes acting on a prismatic float, it is nevertheless of great importance in determining the total force since it is one of the factors that govern the degree of immersion of the float as a whole and, therefore, the number of flow planes in contact with the seaplane bottom at any instant. As a result, the time history of the motion of the seaplane is greatly influenced by the magnitude of the component of velocity parallel to the keel and is governed not only by the amount of momentum transmitted to the water directly in contact with the float but by the manner in which the momentum lost by the float is distributed between the virtual mass beneath the keel and the downwash behind the step.

The analysis of the impact process is therefore seen to require the determination, on a two-dimensional basis, of the virtual mass associated with the immersed cross sections of the float. The instantaneous magnitude of the two-dimensional virtual mass associated with a given float cross section may be expressed in terms of the mass of water contained in a semicylinder of unit length corresponding to the disturbed fluid on one side of an equivalent plate or ellipse in submerged motion. In potential flow, since the virtual mass of a float cross section is determined by the immersed shape, the diameter of the semicylinder is a function of the penetration z. For curved or

irregularly shaped cross sections, the virtual mass may be approximated by means of Wagner's expanding-plate analogy (reference 2). In reference 3 the variation of virtual mass with penetration calculated by application of this theory was employed in the analysis of impacts of a scalloped-bottom float. In the case of V-shaped cross sections, however, if the chines are not immersed, the flow patterns at all degrees of penetration are models of each other and the diameter of the associated semicylinder of water will be directly proportional to the penetration. The constant of proportionality is determined by the dead-rise angle β. The two-dimensional virtual mass of any V-shaped cross section may, therefore, be defined as

$$m_w = \left[f(\beta)\right]^2 \frac{\rho\pi}{2} z^2 \tag{1}$$

where the quantity $f(\beta)z$ represents the radius of the equivalent semicylinder of water associated with the immersed shape.

The correction factor representing the reduction in total force due to finite aspect ratio in the three-dimensional case may, for the present, be written as $\phi(A)$.

Since the quantities $f(\beta)$ and $\phi(A)$ are constant during an impact, their numerical values do not affect the mathematical derivation or the general solutions of the equations of motion, which may therefore be carried out with the foregoing functional notation. In a subsequent section of this paper quantitative expressions for the dead-rise variation and the end-flow correction will be presented and discussed in order to permit direct application of the theoretical results to the prediction of the forces and motions experienced by any given V-bottom seaplane during a step impact.

Resolution of the Problem

Instantaneous force equation.- On the basis of the foregoing theoretical concepts, the motion of a V-bottom seaplane is analyzed for the step-impact condition. The analysis applies equally to a first impact or to a subsequent impact occurring after the seaplane has rebounded from the water surface, provided that the initial conditions are taken at the beginning of the impact under consideration. Since conventional floats and hulls are essentially prismatic for an appreciable distance forward of the step, the analysis is carried out under the assumption that the immersed part of the float has constant cross section. The trim of the float is assumed to remain constant during the short duration of the impact.

Figure 1 is a schematic representation of a prismatic float in the process of immersion at positive trim. The water beneath the float is considered divided into flow planes which are fixed in space and oriented normal to the keel. A given flow plane is specified by the distance s from the foremost immersed station along the keel. The penetration into a fixed flow plane is denoted by z. The penetration of the step is designated by the dimension z_s, which moves with the float. The draft y is a projection of z_s normal to the water surface and is equal to $z_s \cos \tau$.

In accordance with the previous discussion, the momentum imparted to the fluid in a given flow plane is

$$h = m_w \dot{z}\, ds$$

$$= \left[f(\beta)\right]^2 \frac{\rho\pi}{2} z^2 \dot{z}\, ds \tag{2}$$

The reaction of the fluid in the plane to the motion of the float is therefore

$$dF = \left[f(\beta)\right]^2 \frac{\rho\pi}{2}\left(z^2\ddot{z} + 2z\dot{z}^2\right) ds \tag{3}$$

The total force on the float, which acts normal to the keel, is obtained by integrating along the length and applying the reduction factor $\phi(A)$ as a correction for end losses.

Since $z = s \tan \tau$, the total force on the float at any instant is given by

$$F = \left[f(\beta)\right]^2 \phi(A) \frac{\rho\pi}{2}\left(\ddot{z} \tan^2\tau \int_0^{z_s/\tan\tau} s^2\, ds + 2\dot{z}^2 \tan\tau \int_0^{z_s/\tan\tau} s\, ds\right)$$

or

$$F = \left[f(\beta)\right]^2 \phi(A) \frac{\rho\pi}{2 \tan\tau}\left(\frac{z_s^3 \ddot{z}}{3} + z_s^2 \dot{z}^2\right) \tag{4}$$

Equation (4), which corresponds to equation (22) of reference 1, provides the relationship between the total force on the float and the instantaneous state of motion. With $\ddot{z}$ set equal to zero, this equation likewise applies to the problem of steady state planing.

Equations of motion during impact.- Treating the seaplane as a free body and employing equation (4) permit the determination of the motion characteristics of the impact by application of Newton's second law. The assumption of constant wing lift equal to the weight of the seaplane results in the equation of motion

$$-\frac{W}{g}\ddot{z} = \left[f(\beta)\right]^2 \phi(A) \frac{\rho\pi}{2 \tan \tau}\left(\frac{z_s^3\ddot{z}}{3} + z_s^2\dot{z}^2\right) \tag{5}$$

which expresses the general relationship that exists among the variables at any time during the impact process.

For convenience in comparing the theoretical results with experimental data obtained in laboratory testing, equation (5) may be rewritten in terms of the coordinate system relative to the water surface. The transformation of equation (5) requires the application of the respective relationships between z_s, $\dot{z}$, $\ddot{z}$ and y, $\dot{y}$, $\ddot{y}$. From figure 1 it can be readily seen that the normal velocity component $\dot{z}$ and the component parallel to the keel V_p are related to the horizontal and vertical velocity components $\dot{x}$ and $\dot{y}$ by the expressions

$$\dot{z} = \dot{x} \sin \tau + \dot{y} \cos \tau \tag{6}$$

and

$$V_p = \dot{x} \cos \tau - \dot{y} \sin \tau \tag{7}$$

Since the resultant acceleration is normal to the keel,

$$\ddot{z} = \frac{\ddot{y}}{\cos \tau} \tag{8}$$

and there is no longitudinal acceleration in the direction parallel to the keel. Thus V_p is at all times constant and equal to its initial value at contact:

$$V_p = \dot{x}_o \cos \tau - \dot{y}_o \sin \tau$$

$$= \dot{x} \cos \tau - \dot{y} \sin \tau \tag{9}$$

Combining equations (6) and (9) gives

$$\dot{z} = \frac{\dot{y}}{\cos \tau} + K \tag{10}$$

where

$$K = V_p \tan \tau$$

$$= \left(\dot{x}_o - \dot{y}_o \tan \tau\right) \sin \tau \tag{11}$$

Substitution of equations (8) and (10), together with the geometric relationship $z_s = \frac{y}{\cos \tau}$, in equation (5) results in the transformed equation of motion that relates the motion variables with respect to the coordinate system relative to the water surface:

$$-\frac{W}{g}\ddot{y} = \frac{\left[f(\beta)\right]^2 \phi(A) \rho \pi}{6 \sin \tau \cos^2 \tau}\left[y^3 \ddot{y} + 3y^2(\dot{y} + K \cos \tau)^2\right] \tag{12}$$

or

$$\left[1 + \left(\frac{\alpha g}{W}\right) y^3\right]\ddot{y} + 3\left(\frac{\alpha g}{W}\right) y^2(\dot{y} + K \cos \tau)^2 = 0 \tag{12a}$$

where

$$\alpha = \frac{\left[f(\beta)\right]^2 \phi(A) \rho \pi}{6 \sin \tau \cos^2 \tau}$$

Integration of equation (12a) provides the relationship between the draft and vertical velocity:

$$\frac{\left[1 + \left(\frac{\alpha g}{W}\right) y^3\right](\dot{y} + K \cos \tau) e^{\left(\frac{K \cos \tau}{\dot{y} + K \cos \tau} - \frac{K \cos \tau}{\dot{y}_o + K \cos \tau}\right)}}{\dot{y}_o + K \cos \tau} - 1 = 0 \tag{13}$$

The preceding equations apply throughout the impact process.

From equations (12a) and (13), it can be seen that the motion experienced by the float during an impact is governed by the three constants $\left(\frac{\alpha g}{W}\right)$, K cos τ, and $\dot{y}_o$. Thus, for given values of these quantities, identical float motions will be obtained regardless of the separate magnitudes of the primary variables.

The quantity α, which is determined by the shape of the immersed volume, is a factor such that αy^3 represents the instantaneous three-dimensional virtual mass associated with the submerged portion of the float bottom. The virtual mass is expressed in the form of a half-cone of water constituting the summation of the two-dimensional semicircular increments of virtual mass in the individual flow planes and is modified by the aspect-ratio reduction factor $\phi(A)$. The magnitude of the constant $\left(\frac{\alpha g}{W}\right)$ therefore determines the ratio of the virtual mass at any draft to the mass of the float.

The expression K cos τ represents the vertical component of velocity due to motion of the float parallel to the keel. This component, which is constant during an impact, causes the immersed float volume for a given displacement of the float in the direction perpendicular to the keel to be less than that which would exist in the case where there is no longitudinal velocity component. As a result, there is a smaller virtual mass acting on the float and a loss of momentum to the downwash behind the step. In an impact where the resultant velocity is normal to the keel, since the total momentum lost by the float is contained solely within the flow planes in contact with the bottom, the instantaneous velocity at any draft is determined by the ratio of the virtual mass to the float mass. When the path of motion of the seaplane is inclined to the keel, however, as a result of the loss of momentum to the downwash, the ratio of the virtual mass to the float mass is not alone sufficient to determine the instantaneous velocity since, in this case, only part of the momentum lost by the float is included within the virtual mass beneath the float. Thus, as previously noted, although the instantaneous hydrodynamic force is determined solely by the penetration of the float and the components of velocity and acceleration normal to the keel, the time history of the float motion is seen to depend, in addition, on the manner in which the momentum lost by the float is distributed between the virtual mass beneath the keel and the downwash resulting from motion of the float parallel to its axis.

Dimensionless representation of impact characteristics.- Since the behavior of the float during an impact is dependent upon a large number of variables constituting the float properties, such as weight and shape, as well as the attitude and state of motion at initial contact, a nondimensional treatment of the motion may be employed in order to decrease the number of independent variables which must be considered. This approach permits the time histories of the seaplane motions and

loads for different conditions to be reduced to a common basis; thus, fewer solutions are required to cover the entire range of seaplane and flight parameters and the presentation of the theoretical and experimental results is simplified.

By rearrangement of the equations of motion, dimensionless variables may be formed which are related at all instants during the impact by a single parameter κ, which is a function solely of the trim and the initial flight-path angle relative to the water surface. Thus, by applying equation (12a), the nondimensional load-factor coefficient C_l is shown to be related to the instantaneous vertical-velocity ratio $\dot{y}/\dot{y}_o$ and the draft coefficient C_d by the expression

$$C_l = -\frac{\ddot{y}}{\dot{y}_o^2}\left(\frac{W}{\alpha g}\right)^{1/3}$$

$$= \frac{3\left[y^3\left(\frac{\alpha g}{W}\right)\right]^{2/3}\left(\frac{\dot{y}}{\dot{y}_o}+\kappa\right)^2}{1+y^3\left(\frac{\alpha g}{W}\right)} \qquad (14)$$

where $\left[y^3\left(\frac{\alpha g}{W}\right)\right]^{1/3}$ is the draft coefficient and the parameter κ is the quantity $\frac{K\cos\tau}{\dot{y}_o}$.

The load-factor coefficient may also be written in the following equivalent forms:

$$C_l = \frac{n_{l_w}}{\dot{y}_o^2}\left(\frac{Wg^2}{\alpha}\right)^{1/3}$$

$$= \frac{n_{l_w} g}{\dot{y}_o^2}\left(\frac{W}{g}\left\{\frac{6\sin\tau\cos^2\tau}{\left|f(\beta)\right|^2\phi(A)\rho\pi}\right\}\right)^{1/3} \qquad (15)$$

where the impact load factor is defined by $n_{l_w} = -\frac{\ddot{y}}{g}$.

In a similar manner equation (13) may be rewritten to obtain the relationship between the nondimensional draft coefficient and the vertical-velocity ratio:

$$C_d = y\left(\frac{\alpha g}{W}\right)^{1/3} = \left\{ \frac{(1+\kappa)}{\left(\frac{\dot{y}}{\dot{y}_o}+\kappa\right)} e^{\kappa\left[\frac{1}{(1+\kappa)} - \frac{1}{\left(\frac{\dot{y}}{\dot{y}_o}+\kappa\right)}\right]} - 1 \right\}^{1/3} \tag{16}$$

The draft coefficient may also be written in the equivalent form

$$C_d = y\left(\frac{g}{W}\left\{\frac{\left[f(\beta)\right]^2 \phi(A)\rho\pi}{6 \sin \tau \cos^2\tau}\right\}\right)^{1/3} \tag{17}$$

Combining equations (14) and (16) results in the expression directly relating the load-factor coefficient and the vertical-velocity ratio:

$$C_l = -\frac{\ddot{y}}{\dot{y}_o{}^2}\left(\frac{W}{\alpha g}\right)^{1/3}$$

$$= 3\left(\frac{\dot{y}}{\dot{y}_o}+\kappa\right)^2 \left(\frac{\left(\frac{\dot{y}}{\dot{y}_o}+\kappa\right)}{(1+\kappa)} e^{\kappa\left[\frac{1}{\left(\frac{\dot{y}}{\dot{y}_o}+\kappa\right)} - \frac{1}{(1+\kappa)}\right]} \left\{ 1 - \frac{\left(\frac{\dot{y}}{\dot{y}_o}+\kappa\right)}{(1+\kappa)} e^{\kappa\left[\frac{1}{\left(\frac{\dot{y}}{\dot{y}_o}+\kappa\right)} - \frac{1}{(1+\kappa)}\right]} \right\}^2 \right)^{1/3} \tag{18}$$

and also gives the relationship between the load-factor coefficient and the draft coefficient:

$$\kappa\left\{\frac{1}{1+\kappa}-\frac{y\left(\frac{\alpha g}{W}\right)^{1/3}}{\sqrt{-\frac{1}{3}\frac{\ddot{y}}{\dot{y}_o{}^2}\left(\frac{W}{\alpha g}\right)^{1/3}\left[1+y^3\left(\frac{\alpha g}{W}\right)\right]}}\right\}$$

$$+\log_e\frac{(1+\kappa)y\left(\frac{\alpha g}{W}\right)^{1/3}}{\sqrt{-\frac{1}{3}\frac{\ddot{y}}{\dot{y}_o{}^2}\left(\frac{W}{\alpha g}\right)^{1/3}\left[1+y^3\left(\frac{\alpha g}{W}\right)\right]^3}}=0 \qquad (19)$$

In the preceding equations

$$\kappa=\frac{K\cos\tau}{\dot{y}_o}$$

$$=\frac{\dot{x}_o}{\dot{y}_o}\sin\tau\cos\tau-\sin^2\tau$$

The initial horizontal and vertical components of velocity are related to the flight-path angle at contact γ_o by the expression

$$\frac{\dot{y}_o}{\dot{x}_o}=\tan\gamma_o$$

Therefore

$$\kappa=\cot\gamma_o\sin\tau\cos\tau-\sin^2\tau$$

$$=\frac{\sin\tau}{\sin\gamma_o}\cos(\tau+\gamma_o) \qquad (20)$$

The foregoing equations show that the instantaneous magnitudes of the nondimensional variables are related to each other at all instants during the course of an impact by the parameter κ which is determined

by the initial conditions τ and γ_o. Since all coefficients at the same instant are uniquely related through κ, the simultaneous values of the draft coefficient and the load-factor coefficient may be calculated for each instant throughout the impact by assuming successively smaller values of the vertical-velocity ratio $\frac{\dot{y}}{\dot{y}_o} \leq 1$. By this procedure the motion of the seaplane is defined from the instant of initial contact until the occurrence of the rebound from the water surface.

For a given value of κ, therefore, the respective variations during the impact of the nondimensional draft coefficient, vertical-velocity ratio, and load-factor coefficient may each be represented by a single curve regardless of what the seaplane properties, attitude, or initial conditions may be. Consequently, a single variation of κ exists for each of the dimensionless variables representing the state of motion and the time at any given stage of the impact. The use of dimensionless coefficients, by thus taking into account such factors as dead rise, weight, trim angle, and velocity in accordance with the laws governing the variation of the motion with these quantities, permits reduction of all time histories for the same approach parameter to a common basis. As a result, the number of solutions required to cover the entire range of seaplane and flight variables is greatly decreased. In addition, the presentation of both theoretical and experimental results is simplified and a basis is provided for the ready correlation of large quantities of data obtained under diverse conditions.

A graph of κ in terms of the trim and initial flight-path angle is presented in figure 2. For research purposes, laboratory tests may be made at values of κ ranging from zero for impacts where the resultant velocity is normal to the keel $\left(\gamma_o = 90^\circ - \tau;\ \text{near-vertical-drop condition}\right)$ to values approaching infinity at the planing condition. In smooth water, γ_o and τ are referred to the horizontal plane. As indicated in reference 3, the motion of the seaplane in rough water may be approximated by rotating the axes and taking the initial conditions relative to the wave surface. Although statistical data showing the frequency of occurrence of the initial conditions encountered in normal seaplane operations are, unfortunately, not available, the practical range of the approach parameter for conventional seaplanes may be considered limited to values between 0.2 and 10.

On the basis of the equations presented in this section, figures 3, 4, and 5 show the calculated variation of the motion coefficients throughout the impact for several values of κ. These curves cover a greater range of initial conditions than is usually encountered in normal seaplane operations.

As seaplanes become larger and more flexible, the time characteristics of the motion during landing become of increasing significance in determining the dynamic response of the structure. Similarly, in experimental

research the design of suitable instrumentation is greatly aided by knowledge of the time-history characteristics of the quantities to be measured. Because of the nature of the equations of motion, a direct analytical solution in terms of time has not been obtained. However, the use of numerical or graphical methods for integrating the relationships between the variables during the impact permits the ready determination of the time after initial contact at which each set of the motion coefficients exists. The time may be expressed in the form of a nondimensional time coefficient

$$C_t = \int_0^{C_d} \frac{\dot{y}_o}{\dot{y}} \, dC_d$$

or

$$C_t = \int_1^{\dot{y}/\dot{y}_o} \frac{1}{C_l} \, d\frac{\dot{y}}{\dot{y}_o}$$

where

$$C_t = t\dot{y}_o\left(\frac{\alpha g}{W}\right)^{1/3}$$

$$= t\dot{y}_o\left(\frac{g}{W}\left\{\frac{\left[f(\beta)\right]^2 \phi(A) \rho \pi}{6 \sin \tau \cos^2 \tau}\right\}\right)^{1/3} \qquad (21)$$

The calculation of the time coefficient corresponding to the simultaneous values of $\dot{y}/\dot{y}_o$, C_d, and C_l which exist at any instant during the immersion completes the determination of the motion characteristics of the impact. Figures 6 to 8 show theoretical time histories of the motion variables from the instant of initial contact until the float leaves the water surface, for several values of κ which represent a wide range of initial conditions.

In applying figures 3 to 8 to particular problems involving intermediate values of κ, interpolation of the calculated curves should provide sufficient accuracy for practical purposes. The interpolation of the load-factor curves may be facilitated by the construction of a

graph of $\frac{C_l}{C_{l_{max}}} = \frac{\ddot{y}}{\ddot{y}_{max}}$ against $\frac{C_t}{C_t\left(C_{l_{max}}\right)} = \frac{t}{t\left(\ddot{y}_{max}\right)}$ to be used in conjunction with curves of C_l and C_t corresponding to the instant of maximum acceleration.

Laws of variation.– The preceding analysis has shown that the motion and time characteristics of an impact are completely determined by the approach parameter κ, which is a function of the trim and the initial flight-path angle. Thus, for a given value of κ, since the instantaneous value of the vertical-velocity ratio $\dot{y}/\dot{y}_o$ determines the values of the ratio of virtual mass to float mass, $C_d{}^3 = \left(\frac{\alpha g}{W}\right)y^3$, the load-factor coefficient $C_l = -\frac{\ddot{y}}{\dot{y}_o{}^2}\left(\frac{W}{\alpha g}\right)^{1/3}$, and the time coefficient $C_t = t\dot{y}_o\left(\frac{\alpha g}{W}\right)^{1/3}$ corresponding to the same instant, the respective variations of the dimensionless motion coefficients during the impact may each be represented by a single curve, the shape of which is determined by κ. The quantities $\left(\frac{\alpha g}{W}\right)$ and $\dot{y}_o$ may be considered to serve as scale factors which permit the reduction of the variables to a common basis.

For a given value of κ, therefore, the absolute values of the load factor (acceleration), draft, and time corresponding to a particular stage of the impact process (a given value of $\dot{y}/\dot{y}_o$), such as the instant of maximum acceleration, maximum draft, rebound, or any other proportional part of the immersion process, are related to the primary variables by the following simple proportionalities:

The acceleration corresponding to a given stage of the impact varies in accordance with the relationships:

$$\ddot{y} \propto \dot{y}_o^2$$

$$\propto \left(\frac{W}{g}\right)^{-1/3}$$

$$\propto \left[f(\beta)\right]^{2/3}$$

$$\propto \left[\phi(A)\right]^{1/3}$$

$$\propto \rho^{1/3}$$

$$\propto \left(\sin \tau \cos^2 \tau\right)^{-1/3}$$

The vertical velocity at any instant is directly proportional to the initial vertical velocity.

The draft at any given stage of the impact varies as follows:

$$y \propto \left(\frac{W}{g}\right)^{1/3}$$

$$\propto \left[f(\beta)\right]^{-2/3}$$

$$\propto \left[\phi(A)\right]^{-1/3}$$

$$\propto \rho^{-1/3}$$

$$\propto \left(\sin \tau \cos^2 \tau\right)^{1/3}$$

and is independent of the magnitude of the initial velocity.

The time after contact at which a particular phase of the impact occurs varies in accordance with the relationships:

$$t \propto \frac{1}{\dot{y}_o}$$

$$\propto \left(\frac{W}{g}\right)^{1/3}$$

$$\propto \left[f(\beta)\right]^{-2/3}$$

$$\propto \left[\phi(A)\right]^{-1/3}$$

$$\propto \rho^{-1/3}$$

$$\propto \left(\sin \tau \cos^2 \tau\right)^{1/3}$$

Since the simultaneous values of C_l, C_d, and C_t, for a given value of κ, are determined by the corresponding instantaneous value of $\dot{y}/\dot{y}_o$, it is evident from the form of the coefficients that the ratio of the drafts at which any two events occur during a given impact (for example, the ratio of the draft at maximum acceleration to the maximum draft) is independent of the properties of the float and the magnitude of the initial velocity and is purely a function of κ. In a similar manner, the ratios of the vertical velocities, accelerations, and times corresponding to different stages of the impact also depend only on κ.

The application of the foregoing proportionalities permits the determination of simple relationships that show how various combinations of the instantaneous variables, which may have significance in particular problems, are affected by variations in the float properties and/or initial conditions. As has already been seen, the simultaneously existing values of the motion and time coefficients are determined by the instant

considered as well as by the value of κ for the impact. For a given instant and a particular value of κ, the variation of several such ratios with the other parameters is given by the following proportionalities:

$$\frac{\ddot{y}}{y} \propto \dot{y}_o{}^2\left(\frac{\alpha g}{W}\right)^{2/3}$$

$$\frac{\ddot{y}}{\dot{y}} \propto \dot{y}_o\left(\frac{\alpha g}{W}\right)^{1/3}$$

$$\frac{\ddot{y}}{t} \propto \dot{y}_o{}^3\left(\frac{\alpha g}{W}\right)^{2/3}$$

$$\frac{\dot{y}}{y} \propto \dot{y}_o\left(\frac{\alpha g}{W}\right)^{1/3}$$

$$\frac{\dot{y}}{t} \propto \dot{y}_o{}^2\left(\frac{\alpha g}{W}\right)^{1/3}$$

$$\frac{y}{t} \propto \dot{y}_o$$

The ratio y/t is independent of the float properties. In a similar manner, the dependence of any other combinations of the instantaneous variables on the initial conditions and float properties may be readily determined from the form of the coefficients. The variation with dead rise, trim, and fluid density may be obtained from the definition of α.

Special Conditions

Conditions at maximum acceleration.— Of primary interest to the designer are the maximum loads to which the seaplane will be subjected during a given impact and the variation of these loads with the properties of the seaplane and the flight conditions which may be expected.

Differentiating equation (12a), which applies at all instants during the impact, and setting the third derivative equal to zero gives

an equation that relates the instantaneous load-factor coefficient, draft coefficient, and velocity ratio at the time of maximum acceleration:

$$-\frac{\ddot{y}}{\dot{y}_o^2}\left(\frac{W}{\alpha g}\right)^{1/3} = \frac{\frac{\dot{y}}{\dot{y}_o}\left(\frac{\dot{y}}{\dot{y}_o}+\kappa\right)\left[2-y^3\left(\frac{\alpha g}{W}\right)\right]}{2\left[y^3\left(\frac{\alpha g}{W}\right)\right]^{1/3}\left[1+y^3\left(\frac{\alpha g}{W}\right)\right]} \tag{22}$$

Equating equations (22) and (14) results in the relationship between the velocity ratio and the draft coefficient at maximum acceleration:

$$\frac{\dot{y}}{\dot{y}_o} = \frac{6\kappa\, y^3\left(\frac{\alpha g}{W}\right)}{2-7y^3\left(\frac{\alpha g}{W}\right)} \tag{23}$$

or

$$y^3\left(\frac{\alpha g}{W}\right) = \frac{2\frac{\dot{y}}{\dot{y}_o}}{7\frac{\dot{y}}{\dot{y}_o}+6\kappa} \tag{23a}$$

By substitution in equation (22), the maximum load-factor coefficient may be expressed in terms of the draft coefficient at the instant of maximum acceleration by

$$-\frac{\ddot{y}}{\dot{y}_o^2}\left(\frac{W}{\alpha g}\right)^{1/3} = \frac{3\kappa^2\left[y^3\left(\frac{\alpha g}{W}\right)\right]^{2/3}\left[2-y^3\left(\frac{\alpha g}{W}\right)\right]^2}{\left[2-7y^3\left(\frac{\alpha g}{W}\right)\right]^2\left[1+y^3\left(\frac{\alpha g}{W}\right)\right]} \tag{24}$$

or, in terms of the vertical-velocity ratio at the same instant, by

$$-\frac{\ddot{y}}{\dot{y}_o^2}\left(\frac{W}{\alpha g}\right)^{1/3} = \frac{2\frac{\dot{y}}{\dot{y}_o}\left(\frac{\dot{y}}{\dot{y}_o}+\kappa\right)^2}{3\frac{\dot{y}}{\dot{y}_o}+2\kappa}\left(\frac{7\frac{\dot{y}}{\dot{y}_o}+6\kappa}{2\frac{\dot{y}}{\dot{y}_o}}\right)^{1/3} \tag{25}$$

Combining expressions (16) and (23) results in an equation which relates the draft coefficient at the instant of maximum acceleration and the approach parameter κ:

$$\frac{y^3\left(\frac{\alpha g}{W}\right)(6\kappa+7)-2}{(1+\kappa)\left[2-y^3\left(\frac{\alpha g}{W}\right)\right]} = \log_e \frac{\kappa\left[2-y^3\left(\frac{\alpha g}{W}\right)\right]\left[1+y^3\left(\frac{\alpha g}{W}\right)\right]}{(1+\kappa)\left[2-7y^3\left(\frac{\alpha g}{W}\right)\right]} \tag{26}$$

The relationship between the vertical-velocity ratio at the instant of maximum acceleration and κ is obtained by equating equations (16) and (23a):

$$\kappa\left[\frac{1}{(1+\kappa)}-\frac{1}{\frac{\dot{y}}{\dot{y}_o}+\kappa}\right] = \log_e \frac{\left(9\frac{\dot{y}}{\dot{y}_o}+6\kappa\right)\left(\frac{\dot{y}}{\dot{y}_o}+\kappa\right)}{\left(7\frac{\dot{y}}{\dot{y}_o}+6\kappa\right)(1+\kappa)} \tag{27}$$

The analytical solution of equation (26) or (27) for $y^3\left(\frac{\alpha g}{W}\right)$ or $\dot{y}/\dot{y}_o$ and substitution in equations (24) and (25) would provide the separate relationships between κ and the draft coefficient, vertical-velocity ratio, and load-factor coefficient, respectively, at the instant of maximum acceleration. However, although equations (26) and (27) have not been solved analytically, numerical or graphical methods may be employed to determine the magnitude of the variables at the instant of maximum acceleration.

In figures 9(a), (b), and (c), the calculated values of C_d, $\dot{y}/\dot{y}_o$, and C_l at maximum acceleration are plotted against κ for a wide range of approach conditions. The time coefficient at maximum acceleration C_t, which was calculated for given values of κ by integrating the relationship between the variables in the manner previously discussed is shown as a function of κ in figure 9(d).

Conditions at maximum draft.— Explicit solutions may be obtained for the maximum draft coefficient and the load-factor coefficient at maximum draft as functions of κ. At the instant of maximum draft, $\frac{\dot{y}}{\dot{y}_o} = 0$. Therefore, the application of equation (16), gives

$$y\left(\frac{\alpha g}{W}\right)^{1/3} = \left(\frac{1+\kappa}{\kappa} e^{-\frac{1}{1+\kappa}} - 1\right)^{1/3} \tag{28}$$

In addition to the maximum draft, the maximum wetted keel length may be determined from equation (28) by means of the substitution $l = \frac{y}{\sin\tau}$.

The load-factor coefficient at the instant of maximum draft is obtained from equation (18):

$$-\frac{\ddot{y}}{\dot{y}_o^2}\left(\frac{W}{\alpha g}\right)^{1/3} = \frac{3\kappa^2}{1+\kappa}\left(\kappa e^{\frac{1}{1+\kappa}}\right)^{1/3}\left[(1+\kappa) - \kappa e^{\frac{1}{1+\kappa}}\right]^{2/3} \tag{29}$$

Figures 9(a) and (c) present graphs of equations (28) and (29) showing the variation of C_d and C_l at maximum draft with κ. Calculated values of the time coefficient C_t corresponding to maximum draft are presented in figure 9(d).

Conditions at rebound.— The impact process is completed when the float finally leaves the water surface and rebounds into the air. At this instant, $y = 0$ and, if the wing lift is still assumed to be constant and equal to the weight, $\ddot{y} = 0$. Therefore, by applying

equation (16), the vertical-velocity ratio at rebound can be related to the approach parameter by the expression

$$\left(\frac{\dot{y}}{\dot{y}_o}+\kappa\right)e^{\left(\frac{\kappa}{\frac{\dot{y}}{\dot{y}_o}+\kappa}\right)}=(1+\kappa)e^{\frac{\kappa}{1+\kappa}} \tag{30}$$

Figure 9(b) presents the variation with κ of the vertical-velocity ratio at the instant of rebound, as determined from equation (30). The corresponding time coefficient is shown in figure 9(d).

Limiting conditions.- Since the approach parameter κ may range between 0 and ∞, it is desirable to determine the limiting values between which the coefficients of motion at different stages of the impact may vary. The condition of $\kappa = 0$ is obtained when the flight path at contact is normal to the keel of the float. Applying equations (14) and (16) gives the equations of motion for this case

$$-\frac{\ddot{y}}{\dot{y}_o^2}\left(\frac{W}{\alpha g}\right)^{1/3}=\frac{3\left[y^3\left(\frac{\alpha g}{W}\right)\right]^{2/3}\left(\frac{\dot{y}}{\dot{y}_o}\right)^2}{1+y^3\left(\frac{\alpha g}{W}\right)} \tag{31}$$

and

$$y^3\left(\frac{\alpha g}{W}\right)=\frac{1-\frac{\dot{y}}{\dot{y}_o}}{\frac{\dot{y}}{\dot{y}_o}} \tag{32}$$

Since αy^3 represents the virtual mass, equation (32) shows that the sum of the instantaneous momentum of the float and the momentum of the water directly beneath the float (virtual mass) is constant throughout the impact and equal to the initial momentum of the float. This equality of momentum exists only when κ is equal to zero. Since the deceleration of the float in this case is in the same direction as the

resultant velocity, the float continues along its original path of motion throughout the impact. Thus, only the flow planes directly beneath the float will be affected by the immersion and will absorb all the momentum lost by the float. For values of κ other than zero, this relationship does not apply since part of the momentum lost by the float will be contained in the fluid left behind as the downwash.

Combining equations (31) and (32) permits the load-factor coefficient to be written in terms of the vertical-velocity ratio or the draft coefficient:

$$-\frac{\ddot{y}}{\dot{y}_o^2}\left(\frac{W}{\alpha g}\right)^{1/3} = 3\left(\frac{\dot{y}}{\dot{y}_o}\right)^{7/3}\left(1 - \frac{\dot{y}}{\dot{y}_o}\right)^{2/3} \tag{33}$$

and

$$-\frac{\ddot{y}}{\dot{y}_o^2}\left(\frac{W}{\alpha g}\right)^{1/3} = \frac{3\left[y\left(\frac{\alpha g}{W}\right)^{1/3}\right]^2}{\left[1 + y^3\left(\frac{\alpha g}{W}\right)\right]^3} \tag{34}$$

The time coefficient may be directly obtained by integrating equation (32):

$$t\dot{y}_o\left(\frac{\alpha g}{W}\right)^{1/3} = y\left(\frac{\alpha g}{W}\right)^{1/3}\left[1 + \frac{1}{4}y^3\left(\frac{\alpha g}{W}\right)\right] \tag{35}$$

Equation (35) shows that the draft always increases with time. Thus, while the downward velocity of the float grows smaller as the impact progresses, a maximum draft is never reached. This result is further evident from the fact that, since the momentum lost by the float is contained in the virtual mass alone, an infinite virtual mass (infinite draft) is required to satisfy the condition of zero vertical velocity. This result is due to the neglect of the buoyant forces which, because of the large drafts involved, are of greatest importance at very steep flight-path angles beyond the range of practical seaplane landing conditions.

Combining equations (32) and (35) gives the relationship between the time coefficient and the vertical-velocity ratio:

$$t\dot{y}_o\left(\frac{\alpha g}{W}\right)^{1/3} = \left(\frac{1 - \frac{\dot{y}}{\dot{y}_o}}{\frac{\dot{y}}{\dot{y}_o}}\right)^{1/3}\left(1 + \frac{1}{4}\,\frac{1 - \frac{\dot{y}}{\dot{y}_o}}{\frac{\dot{y}}{\dot{y}_o}}\right) \tag{36}$$

For $\kappa = 0$, equation (23a) permits the ready determination of the ratio of the virtual mass to the float mass at the instant of maximum acceleration

$$y^3\left(\frac{\alpha g}{W}\right) = \frac{2}{7} \tag{37}$$

Thus the draft coefficient at maximum acceleration is

$$y\left(\frac{\alpha g}{W}\right)^{1/3} = \left(\frac{2}{7}\right)^{1/3} = 0.6586 \tag{38}$$

The vertical-velocity ratio at this instant is obtained from equation (32):

$$\frac{\dot{y}}{\dot{y}_o} = \frac{7}{9} \tag{39}$$

whereas the load-factor coefficient is obtained from equation (31):

$$-\frac{\ddot{y}}{\dot{y}_o{}^2}\left(\frac{W}{\alpha g}\right)^{1/3} = 3\left(\frac{2}{7}\right)^{2/3}\left(\frac{7}{9}\right)^3 = 0.6123 \tag{40}$$

and the time coefficient from equation (35):

$$t\dot{y}_o\left(\frac{\alpha g}{W}\right)^{1/3} = \left(\frac{2}{7}\right)^{1/3}\left(1 + \frac{1}{14}\right) = 0.7057 \qquad (41)$$

For $\kappa = 0$, since a maximum draft is never reached, there will be no reversal of the vertical motion and the float will never leave the water. These results are peculiar to $\kappa = 0$ for the reasons previously stated. At all other values of κ, because of the loss of momentum to the downwash resulting from inclination of the flight path to the keel, a maximum draft will be attained and the float will rebound from the water surface in a finite time. For steep impacts (small values of κ) the difference in time coefficient between the occurrence of maximum acceleration, maximum draft, and rebound will be large. As the flight path becomes flatter this difference becomes smaller until, as the condition of planing ($\kappa = \infty$) is approached, there is no difference. For the latter condition, the motion coefficients approach the following limiting values:

$$\lim_{\kappa \to \infty} C_l = \infty$$

$$\lim_{\kappa \to \infty} \frac{\dot{y}}{\dot{y}_o} = 1$$

$$\lim_{\kappa \to \infty} C_d = 0$$

$$\lim_{\kappa \to \infty} C_t = 0$$

For planing with only partial wing lift the relationship among the variables may be calculated by setting the left-hand member of equation (12) equal to the load on the water and letting $\ddot{y} = \dot{y} = 0$.

Chine immersion.- The foregoing analysis has assumed that the width (beam) of the V-shaped float bottom is sufficiently great that the chines do not become immersed at any time during the impact. Although this condition is generally true for the flight-path angles encountered in normal operation and the range of beam loadings employed in current American seaplane design practice, some mention should be made of the effects of chine immersion accompanying the greater penetrations which may be experienced with more heavily loaded seaplanes and/or steeper flight-path angles.

From the preceding discussion of the physical concepts upon which the analysis is based, it can be seen that the force exerted on a given cross section of the float by the water may be considered to result from two actions; namely, the increase in virtual mass accompanying the enlarging flow pattern and the reaction to the acceleration of the virtual mass $\left(dF = \left(\dot{m}_w\dot{z} + m_w\ddot{z}\right) ds\right)$. In any given flow plane, since the penetration of the chines marks the end of the expansion of the wetted width, in the absence of a more rigorous analysis of the flow, further immersion of the cross section may be assumed to take place with almost constant virtual mass, which results in a decrease in force from that which would exist if the V-shape had continued to grow in width. In the case of the three-dimensional float at positive trim, the reduction in total force should occur gradually as successive stations along the keel, beginning at the step, become immersed beyond the chines during the later stages of the impact.

The possibility of the occurrence of chine immersion during a given impact and its approximate effect on the maximum acceleration may be evaluated from figure 4 by comparing the value of the draft coefficient corresponding to maximum acceleration and the draft coefficient that would exist at the instant of chine immersion. If the wetted width at the step c_s is taken equal to the width of the effective plate corresponding to the virtual mass, the relationship between the wetted semiwidth and the draft is given by

$$c_s = f(\beta) z_s$$

$$= \frac{f(\beta) y}{\cos \tau}$$

Thus, the draft coefficient at the instant of chine immersion is

$$C_{d_{ch}} = \left(\frac{\alpha g}{W}\right)^{1/3} \frac{c_{s_{ch}} \cos \tau}{f(\beta)}$$

$$= c_{s_{ch}} \left[\frac{g}{W}\left(\frac{\phi(A)\rho\pi}{6 f(\beta) \tan \tau}\right)\right]^{1/3} \qquad (42)$$

If $C_{d_{ch}}$ is greater than the draft coefficient at which the maximum load-factor coefficient occurs, there will not be any decrease in the maximum load due to chine immersion. However, if $C_{d_{ch}}$ is less than C_d

corresponding to the maximum load-factor coefficient, then, for practical purposes, the maximum load-factor coefficient may be considered limited to the value of C_l corresponding to $C_{d_{ch}}$.

Equation (26) permits the determination of the largest values of κ (flattest impact conditions) at which a reduction in $C_{l_{max}}$ due to the effects of chine immersion is encountered; that is, the values of κ required to cause the chines to become immersed, for given values of $C_{d_{ch}}$, at the same instant at which the maximum acceleration is reached when there is no chine immersion. For all smaller values of κ (steeper impacts), the variation of the maximum load-factor coefficient with κ, as modified by chine immersion, is determined from equation (19), by letting $C_d = C_{d_{ch}}$. The effect of chine immersion on $C_{l_{max}}$ is shown in figure 10 by the broken-line curves which have been calculated by the aforementioned procedure for several values of $C_{d_{ch}}$ corresponding to a wide range of beam loadings extending from conventional values to beam loadings considerably higher than those employed in present-day design practice.

Evaluation of $f(\beta)$ and $\phi(A)$

Although additional research is still required to define completely the variation of virtual mass with dead rise in the two-dimensional case and to establish further the losses due to finite aspect ratio in the three-dimensional case, sufficient information of both a theoretical and empirical nature is available at present to permit the application of the foregoing analysis to V-bottom seaplanes having conventional dead-rise angles. Analytically, the virtual mass in any flow plane may be evaluated from the results of an iterative solution made by Wagner to calculate the force on a two-dimensional V-shape of 18° angle of dead rise, during immersion at constant velocity. The results for 18° angle of dead rise were extended to other dead-rise angles by equation (78) of reference 2, which, in the terminology of the present paper, may be written as

$$dF = \left(\frac{\pi}{2\beta} - 1\right)^2 \rho \pi z \dot{z}^2 \, ds \tag{43}$$

The virtual mass corresponding to equation (43) may be evaluated by recognizing that, for constant velocity penetration, the force in a given flow plane is due solely to the increase in virtual mass accompanying the enlarging flow pattern. For this condition, equation (3) becomes

$$dF = \left[f(\beta)\right]^2 \rho \pi z \dot{z}^2 \, ds \tag{44}$$

From equations (43) and (44) it is easily seen that

$$f(\beta) = \left(\frac{\pi}{2\beta} - 1\right) \tag{45}$$

Thus

$$m_w = \left(\frac{\pi}{2\beta} - 1\right)^2 \frac{\rho\pi}{2} z^2 \tag{46}$$

is the two-dimensional virtual mass satisfying Wagner's force solution.

The evaluation of the virtual mass permits the determination of the rise of the disturbed water surface in the immediate vicinity of the seaplane above the level-water surface (at infinity). If the virtual mass in any flow plane is expressed in terms of the semicircular mass of water corresponding to the disturbed fluid on one side of a plate in submerged motion

$$m_w = \frac{\rho\pi}{2} c^2$$

$$= \left[f(\beta)\right]^2 \frac{\rho\pi}{2} z^2$$

and

$$c = f(\beta) z$$

where c is the radius of the semicircular virtual mass and is equal to the semiwidth of the plate.

If the wetted width of the V-bottom in any flow plane is assumed equal to the width of the equivalent plate, the equation

$$\frac{r}{z} = f(\beta) \tan \beta - 1 \tag{47}$$

gives the geometrical relationship in a flow plane between the rise of the water surface in contact with the float and the penetration of the float with respect to the undisturbed water surface.

Equations (43) to (47) are valid only as long as the immersed cross section in any flow plane is a V-shape and do not apply after the chines become immersed. In the case of V-shaped cross sections with chine flare, equation (46) holds until the flared portion reaches the water surface, after which Wagner's expanding-plate analogy (reference 2) may be applied to determine the equation of the free surface at the instant of chine immersion and calculate the increase in virtual mass with further immersion. An example of the procedure for determining the variation of the virtual mass of curved cross sections with penetration is given in reference 3 for the case of a scalloped-bottom float.

An approximate correction for the effects of end flow due to finite aspect ratio may be obtained from the results of experiments conducted by Pabst with vibrating plates in water (reference 4). These tests showed that the factor representing the reduction in virtual mass for the three-dimensional case is closely given by the expression

$$\phi(A) = 1 - \frac{1}{2A} \tag{48}$$

where A is the aspect ratio of the equivalent vibrating plate.

For V-bottom floats, if it is assumed that the end-flow correction is determined by the shape of the intersected area in the plane of the water surface, then the application of Pabst's data to the keeled seaplane results in the expression

$$\phi(A) = 1 - \frac{\tan \tau}{2 \tan \beta} \tag{49}$$

Although it is known from unpublished studies of planing data that the dead-rise and end-flow functions given by equations (45) and (49) are questionable for very low angles of dead rise, these functions have been found to be in rather good agreement with experimental data obtained in the Langley impact basin with floats of $22\frac{1}{2}^\circ$ and 30° angles of dead rise (reference 5) as well as with more recent data obtained with a float of 40° angle of dead rise. Present indications lead to the belief that the aforementioned functions may not be too far in error for angles of dead rise as low as 15°, but more definite conclusions in this respect must await the results of further investigation. It would appear, then, that the functions $f(\beta)$ and $\phi(A)$, as given, should be directly applicable to the range of angle of dead rise most likely to be encountered in conventional seaplane practice.

APPLICABILITY AND LIMITATIONS

In view of the fact that the present analysis considers a float of constant cross section, there may be some question regarding the effects of the pulled-up bow and afterbody in applications to conventional floats. Although the longitudinal warping of the float may be taken into account by more complicated equations, it appears that since conventional floats and hulls are essentially prismatic for a considerable distance forward of the step, the bow will not cause any important deviation of the loads from those calculated on the basis of constant cross section for normal impacts at positive trim (reference 6).

The afterbody, on the other hand, may exert a much more pronounced influence on the motion of the seaplane, particularly in laboratory testing where, as is sometimes the case, the trim of the model may be fixed at very high positive angles. Under such conditions the load is taken almost entirely by the afterbody while the forebody may not become immersed to any appreciable degree until after the maximum acceleration has been attained. At the lower trims associated with step impacts, on the other hand, the depth of step, the keel angle of the afterbody, and the relatively high longitudinal velocity apparently combine to shield the afterbody so that it carries very little load in comparison with the forebody.

In flight impacts, even though the landing approach may be made at high trim, the initial contact aft of the step generally results in a downward pitching of the seaplane to the extent that the main impact occurs at reduced trim and corresponds to a forebody impact. The equations presented may thus be considered to represent approximately free-flight impacts at high trim if the initial conditions are taken to correspond with those at the beginning of the main impact.

As a first approach toward the calculation of the behavior of seaplanes in seaway, the preceding analysis may be applied to rough water impacts if the initial conditions are defined relative to the wave surface. For trochoidal waves with large length-amplitude ratio, the wave profile may be simulated by an inclined plane tangent to the surface at the point of contact, which serves as the effective frame of reference for the foregoing equations. These assumptions fail to consider the internal orbital velocities and displacements of the fluid particles within the wave and are therefore approximate. At best, the procedure should be applied only to impacts where the float contacts the wave about halfway between trough and crest for those cases where the trim is equal to or greater than the slope of the wave. In reference 3, the application of these approximations to several rough-water impacts of a scalloped-bottom float yielded calculated results which were in fairly good agreement with experimental data obtained in the Langley impact basin.

COMPARISON OF THEORETICAL RESULTS WITH EXPERIMENTAL DATA

The applicability of the theory to seaplane impacts is illustrated by comparisons with a large quantity of experimental data which has been obtained over a period of time in the Langley impact basin. The tests included a much wider range of trim and flight-path angles than is usually encountered in normal seaplane operations. Although part of the experimental results has been presented in earlier papers (references 5 to 10), some of the data included in the present investigation have not been previously available.

A description of the impact basin and its equipment is given in reference 7. The test data were obtained in smooth water at fixed trim with two float forebody models, M-1 and M-2, which are described in references 7 and 5. These models, which are of all-metal construction, have lines generally similar to the hulls of conventional flying boats except for the absence of chine flare. Model M-1 has an angle of dead rise of $22\frac{1}{2}^\circ$ at the step, whereas model M-2 is of 30° dead rise. More recent data obtained with a float which has an angle of dead rise of 40° at the step are also included in the present report. The tests were run at a number of weights between 1000 and 2700 pounds and include trim angles ranging from 3° to 15°. The range of flight-path angles investigated included virtually all conditions between planing and vertical drop. Wing lift was simulated by the action of a pneumatic cylinder and cam device which was designed to apply a constant upward force to the model equal to the total weight.

During an impact, the motion of the float normal to the water surface was determined by independent time-history measurements of the acceleration, velocity, and draft at the step. Several different NACA accelerometers were used in the course of the testing. These ranged in natural frequency from 12.5 to 26 cycles per second. The velocity and displacement measurements were made by means of variable-resistance slide-wires whose response characteristics have not been completely determined.

Estimates of the precision of the experimental data are tabulated in references 5, 7, 8, 9, and 10. On the basis of these values, most of the basic measurements are believed to be correct within the following limits:

Horizontal velocity, feet per second	± 0.5
Vertical velocity, feet per second	± 0.2
Vertical displacement (draft), feet	± 0.02
Acceleration, g, percent of reading	5 to -10

It should be noted that the accuracies quoted refer to measurements of the maximum values attained by the variables during an impact. On the other hand, measurements of instantaneous values which require the use

of more than one record trace, such as the acceleration at the instant of maximum draft, involve additional errors due to instrument lag and time-correlation difficulties which have not been fully evaluated.

Comparisons between theoretical and experimental time histories of the draft, velocity, and acceleration are presented in figures 6, 7, and 8 for a range of contact conditions extending from very shallow flight paths ($\kappa = 10$) up to extremely steep flight paths normal to the keel ($\kappa = 0$). A typical seaplane impact in smooth water at, for instance, 6° trim, vertical velocity of 3 feet per second, and horizontal velocity of 80 miles per hour would correspond to a value of $\kappa = 4.05$. For a high-speed landing at 150 miles per hour, for example, and the same sinking speed, the flight-path angle is reduced, giving a value of κ of 7.6. A landing into the flank of an oncoming wave, on the other hand, might correspond to a value of κ as low as 0.2.

Although the dimensionless curves permit the complete determination of the motion of a seaplane during an impact regardless of the properties of the seaplane, its attitude, or the state of motion at initial contact, some interpretation of the results is desirable. For impacts at different values of κ, since both the load-factor coefficient and time coefficient are based on the initial vertical velocity, the actual time histories of the load will have the same relative shapes as the dimensionless curves if the vertical velocity is the same for each κ. Thus the curves shown in figure 8 may be interpreted as corresponding to different seaplanes landing with the same sinking speed but with different resultant velocities and therefore varying flight-path angles. For this case the maximum load for the shallow approaches (high resultant velocities) will be greater than that for the steeper flight-path angles and will be attained in a shorter time after contact.

On the other hand, a somewhat different interpretation of the dimensionless curves is obtained when a particular seaplane landing over a range of flight-path angles is considered. In this case the resultant velocity is more or less constant while the sinking speed, which depends largely on piloting technique, may be varied to obtain a range of flight-path angles. As has been previously shown, the acceleration at any proportional part of the impact cycle varies as the square of the initial vertical velocity whereas the corresponding time is inversely proportional to the vertical velocity. If the resultant velocity and the trim angle are held constant, steeper flight paths are associated with the smaller values of κ. As κ becomes smaller, the resulting increase in vertical velocity more than offsets the corresponding reduction in load-factor coefficient and increase in time coefficient. Consequently, the maximum load obtained with constant resultant velocity and trim will be greater for the steeper approaches than at the low flight-path angles and will be attained in a shorter time after contact. As a result, the test data obtained for the highest value of κ shown in the figures ($\kappa = 10.27$), which corresponds to a very shallow impact with low sinking speed, represent measured accelerations of small magnitude in a region where the accuracy of the accelerometer readings is low.

It can be seen from figures 6, 7, and 8 that the agreement between the experimental and calculated time histories is fairly good throughout almost the entire immersion process. Near the very end of the impact, however, just before the float rebounds from the water surface, there is a deviation which indicates the application of an external downward force on the float and causes the rebound to be slightly delayed. In figure 7, where this effect is most clearly visible, the test points corresponding to the instant of rebound have been differentiated by the addition of a flag (\). The extraneous force is apparently contributed by the test equipment and has been attributed to two factors which take effect after the maximum draft has been reached and the float has begun its upward travel: namely, leakage in the pneumatic "lift" cylinder which balances the weight, and friction in the dropping mechanism. As a result of the reduction in hydrodynamic force accompanying the decrease in draft, the effect of the extraneous force on the motion of the float is proportionately greatest just before the float leaves the water surface. On the whole, it may be said that the discrepancies between theory and test data evident from the figures are within the limits of the experimental accuracy provided by the equipment and instrumentation.

Figures 10 to 13 show how the state of motion corresponding to the instants of maximum acceleration, maximum draft, and rebound varies with κ. A comparison between the theoretical and experimental times at which these events occur is given in figure 14. The test data cover a wide range of weights, velocities, and flight-path angles. A flag (/) attached to an experimental point signifies that chine immersion has occurred previous to the instant represented by the point. Logarithmic scales have been used in figures 10 to 14 in order to spread out the test data and emphasize the differences in the states of motion and times corresponding to the various stages of the impact. The extent of this expansion of the data can be evaluated by a comparison with figure 9 which shows the theoretical curves plotted on a linear scale.

Figure 10 shows the variation of the maximum acceleration (load), in nondimensional form, with the approach parameter κ and compares the theoretical results with experimental data obtained with floats of $22\frac{1}{2}^\circ$, 30°, and 40° angles of dead rise. The reduced scatter of the experimental data for 40° angle of dead rise is due to recent improvements in the instrumentation employed in the tests. The solid curve represents the case in which the beam of the seaplane is large enough so that the chines are not immersed at the instant of maximum acceleration. The effect of chine immersion in reducing the maximum acceleration is shown by the broken-line curves, which have been calculated by the method previously discussed, for several values of $C_{d_{ch}}$ (the draft coefficient at the instant of chine immersion) corresponding to a wide range of beam loadings. For a given beam loading, the intersection of the broken-line curve, corresponding to the proper

value of $C_{d_{ch}}$, and the solid curve determines the value of κ above which there is no reduction in load. For values of the beam loading which have been in the past commonly used in American seaplane design practice $\left(\frac{W}{\rho g b^3} < 1\right)$ and normal flight-path angles, the reduction in maximum acceleration due to chine immersion is quite small.

With higher beam loadings, on the other hand, the theory indicates that an appreciable reduction in load may be obtained. For a given seaplane weight, a decrease in beam of 45 percent increases the beam loading six times. For a seaplane with $22\frac{1}{2}^\circ$ angle of dead rise and a beam loading $\frac{W}{\rho g b^3} = 6$, landing at 6° trim, and $\gamma_o = 5^\circ$, $\kappa = 1.18$ and $C_{d_{ch}} = 0.311$. As may be seen from figure 10, for this condition a 30-percent reduction in load is indicated. With still higher beam loadings, even greater reductions are shown by the curves. Such beam loadings are conceivable for hydrodynamic lifting devices such as long narrow hydroflaps which might be employed as landing gear on high-speed aircraft. The use of devices of this type in conjunction with high beam loadings may offer certain advantages since such applications would not only permit reduction of the landing loads but would also allow the loads to be transmitted to the structure at fixed attachment points with resultant alleviation of the necessity of the entire bottom structure being heavy enough to resist the high local water loads which might otherwise occur anywhere on the bottom, as is the case with conventional flying boats. Unfortunately, at the present time sufficient data are not available to verify the theoretical results for the very high beam-loading conditions.

For more conventional beam loadings, on the other hand, a large quantity of experimental data does exist, extending over a range of beam loading of $2\frac{1}{2}$ to 1 and including values somewhat greater than those currently employed. For the great majority of the test conditions the reduction in maximum acceleration, in agreement with the theory, is small or entirely absent.

Figure 11 shows the variation with κ of the load-factor coefficient corresponding to the instant of maximum draft. From the figure it is seen that this quantity is always less than the value at maximum acceleration, which occurs at an earlier time after contact (fig. 14). As might reasonably be expected, the difference in the load-factor coefficient at these two instants is greatest at the high flight-path angles and decreases as the planing condition is approached. Because of lag in the slide-wire measurements which were used to determine the instant of maximum draft, the recorded time at which this stage of the impact occurs is slightly greater than the actual time. As a result,

the accelerations corresponding to the recorded time of maximum draft are somewhat lower than the true values. At the low values of κ the experimental accelerations at the instant of maximum draft are considerably greater than the theoretical values as a combined result of the immersion of the nonprismatic bow section of the float and the action of the buoyant forces, caused by the large penetrations associated with the high flight-path angles. This effect is most pronounced beyond the range of conditions applicable to conventional seaplanes. The importance of the buoyant forces will be discussed subsequently in more detail.

The vertical velocities at the instants of maximum acceleration and rebound are presented in figure 12. The positive velocities corresponding to the occurrence of maximum acceleration show that the motion of the seaplane is still downward at this instant and that the maximum draft has not yet been attained. At the instant of rebound, the seaplane is traveling upward, hence the negative velocities. The scatter evident in the test data is due to the previously mentioned lag in the slide-wire system as well as to the difficulties encountered in correlating the various independent measurements of the motion which are required to establish the time at which each event occurs.

Figure 13 shows the draft at the instant of maximum acceleration in addition to the maximum draft. As might be reasonably expected, all other conditions being equal, the greater drafts occur at the higher flight-path angles. Similarly, the difference between the maximum draft and the draft at the instant of maximum acceleration is greatest at the low values of κ and decreases as the flight-path angle is reduced. As indicated by the form of the draft coefficient, for a given value of κ, the absolute draft at any stage of the impact is independent of the magnitude of the initial velocity. This fact is borne out by the test data which include an eight-to-one velocity range.

Figure 14 shows the time corresponding to the instants of maximum acceleration, maximum draft, and rebound. Here, again, it is seen that the maximum acceleration is attained before the maximum draft is reached, which in turn, naturally takes place before the seaplane rebounds from the surface of the water. In conformity with the results shown in the preceding figures, for the same sinking speed, a greater time is required to reach a given stage of the impact process at the high flight-path angles than for the flatter-approach conditions. In a similar manner, the differences in time between the occurrence of the various stages are greatest for the low values of κ and become very small as the planing condition is approached. The experimental factors which cause the recorded time of maximum draft and rebound to be slightly delayed have been previously enumerated.

An examination of figure 13 reveals that the maximum draft at low values of κ tends to be slightly less than that specified by the theory. This result is apparently due to the combined effects of immersion of the nonprismatic bow section and the action of the buoyant (gravity) forces which cause the downward motion of the seaplane to be arrested at an earlier time. The buoyant forces are, of course,

larger at the instant of maximum draft than at any other time during the impact and are of greatest importance at the high flight-path angles because of the greater drafts reached. In addition, because the vertical velocities of a seaplane are subject to physical and operational limitations, the resultant velocities at the high flight-path angles are so small as to emphasize still further the importance of the buoyant forces in comparison with the inertia forces for such approach conditions. As a result, the experimental accelerations at maximum draft for the high flight-path angles are greater than the theoretical values. Furthermore, the effect of buoyancy at the instant of maximum draft more than overcomes the reduction in force due to chine immersion, which would otherwise result in slightly greater drafts than would be experienced if the beam of the seaplane were great enough to prevent the chines from reaching the water surface.

For the practical range of flight-path angles applicable to conventional seaplanes, on the other hand, the agreement between the theoretical results and the experimental data indicates that the buoyant forces are relatively insignificant.

SUMMARY OF RESULTS

Theoretical.- (1) The preceding analysis of the motions and hydrodynamic loads experienced by a V-bottom seaplane during a step impact with the water surface has shown that the motion and time characteristics of an impact may be represented in generalized form by means of the following dimensionless variables:

Load-factor coefficient

$$C_l = \frac{n_{l_w} g}{\dot{y}_o^2}\left(\frac{W}{g}\left\{\frac{6 \sin\tau \cos^2\tau}{\left[f(\beta)\right]^2 \phi(A) \rho \pi}\right\}\right)^{1/3}$$

Draft coefficient

$$C_d = y\left(\frac{g}{W}\left\{\frac{\left[f(\beta)\right]^2 \phi(A) \rho \pi}{6 \sin\tau \cos^2\tau}\right\}\right)^{1/3}$$

Time coefficient

$$C_t = t\dot{y}_o\left(\frac{g}{W}\left\{\frac{\left[f(\beta)\right]^2\phi(A)\rho\pi}{6\sin\tau\cos^2\tau}\right\}\right)^{1/3}$$

Vertical-velocity ratio

$$\frac{\dot{y}}{\dot{y}_o}$$

It is also shown that the variation of these dimensionless quantities during an impact is governed solely by the magnitude of the approach parameter

$$\kappa = \frac{\sin\tau}{\sin\gamma_o}\cos\left(\tau + \gamma_o\right)$$

The approach parameter is seen to depend only on the trim and the flight-path angle at the instant of initial contact with the water surface and may be considered a criterion of impact similarity. For a given value of κ, the respective variations of the aforementioned dimensionless variables may each be represented by a single curve, regardless of what the angle of dead rise or weight of the seaplane, the attitude, flight-path angle, or initial velocity may be. As a result, there is a single variation with κ of each of the dimensionless variables representing the state of motion and the time at any given stage of the impact.

(2) For a given value of κ, the draft, load factor, and time corresponding to a given stage of the impact $\left(\text{given value of } \frac{\dot{y}}{\dot{y}_o}\right)$ are related to the primary variables constituting the float properties, attitude, and magnitude of the initial velocity by the following proportionalities:

$$y \propto \left(\frac{W}{g}\left\{\frac{\sin\tau\cos^2\tau}{\left[f(\beta)\right]^2\phi(A)\rho}\right\}\right)^{1/3}$$

$$n_{i_w} \propto \frac{\dot{y}_o^2}{g}\left(\frac{g}{W}\left\{\frac{\left[f(\beta)\right]^2 \phi(A)\rho}{\sin\tau \cos^2\tau}\right\}\right)^{1/3}$$

$$t \propto \frac{1}{\dot{y}_o}\left(\frac{W}{g}\left\{\frac{\sin\tau \cos^2\tau}{\left[f(\beta)\right]^2 \phi(A)\rho}\right\}\right)^{1/3}$$

(3) A study of the variation of the hydrodynamic loads experienced during step impacts shows that:

(a) The maximum acceleration always occurs before the maximum draft is reached.

(b) For a given resultant velocity, if the seaplane properties and attitude remain the same, the accelerations at the high flight-path angles are greater than those at the low flight-path angles and are attained in a shorter time after contact.

(c) For a given sinking speed, on the other hand, greater accelerations are obtained at the low flight-path angles.

(d) The difference between the magnitudes of the maximum load-factor coefficient and the load-factor coefficient at the instant of maximum draft is greatest at high flight-path angles and decreases as the planing condition is approached.

(4) An analysis of the variation of the draft during step impacts shows that:

(a) As indicated by the form of the draft coefficient, the absolute value of the draft at any given stage of the impact is independent of the magnitude of the initial velocity.

(b) All other factors being equal, the greatest drafts occur at the higher flight-path angles.

(c) The difference between the maximum draft and the draft at the instant of maximum acceleration is greatest at high flight-path angles and decreases as the planing condition is approached.

(5) An investigation of the time characteristics of step impacts indicates that:

(a) For a given resultant velocity, if the seaplane properties and attitude remain the same, a greater time is required to reach a given stage of the impact process at the low flight-path angles than is required at the high flight-path angles.

(b) For a given sinking speed, on the other hand, the time to reach a given stage of the impact is greatest at the high flight-path angles.

(c) The difference in the time coefficients corresponding to the occurrence of the various stages of the impact (for example, maximum acceleration, maximum draft, rebound) is greatest at the high flight-path angles and decreases as the planing condition is approached.

(6) For conventional beam loadings and flight conditions the reduction in maximum acceleration due to chine immersion is either small or entirely absent. However, for higher beam loadings than those employed in current design practice, considerable reductions in load can be expected.

Experimental.- Comparison of the theoretical results with test data obtained over a wide range of initial conditions with floats of $22\frac{1}{2}^\circ$, 30°, and 40° angles of dead rise indicates that:

(1) Within the limits of experimental error, the theory provides a good representation of the motion and time variations during the entire impact process, from initial contact until the instant of rebound from the water surface.

(2) For conventional beam loadings and flight conditions, the effects of chine immersion on the maximum acceleration of the seaplane are either small or entirely absent. For higher beam loadings and/or steeper flight-path angles, immersion of the chines, in agreement with the theoretical results, appears to cause appreciable load reductions.

(3) For impacts within the practical range of flight conditions encountered in normal seaplane operation the effects of buoyancy are small. At extremely high flight-path angles, on the other hand, because of the large drafts reached and the fact that the sinking speeds are subject to physical and operational limitations, the effect of buoyancy on the state of motion at the instant of maximum draft is appreciable. Even for such steep flight paths, however, the buoyant forces do not become important until after the maximum acceleration has been attained.

CONCLUDING REMARKS

A theoretical investigation has been made of the motions and hydrodynamic impact loads experienced by V-bottom seaplanes for the step-landing condition. The analysis shows that the motion and time characteristics of an impact may be represented in generalized form by means of dimensionless variables respectively designated the load-factor coefficient, draft coefficient, vertical-velocity ratio, and time coefficient. It is further shown that the variation of these dimensionless quantities during the course of an impact is governed by the magnitude of the approach parameter κ which depends only on the trim and the flight-path angle at the instant of initial contact with the water surface and which may be considered a criterion of impact similarity. As a result of this generalized treatment the number of independent variables and the number of cases for which solutions are required are considerably reduced while the presentation of theoretical and experimental results is greatly simplified; thus, ready correlation of data for the complete range of seaplane and flight parameters is permitted.

The results of the investigation are presented in the form of dimensionless curves which may be used to predict the behavior of V-bottom seaplanes at all instants during an impact as well as at the particular instants of maximum acceleration, maximum draft, and rebound. A comparison of the calculated results with extensive experimental data obtained at the Langley impact basin with floats which have $22\frac{1}{2}^\circ$, 30°, and 40° angles of dead rise indicates that, within the limits of experimental accuracy, the theory provides a good representation of the seaplane motion and the hydrodynamic loads experienced during the course of a step-landing impact.

Langley Memorial Aeronautical Laboratory
National Advisory Committee for Aeronautics
Langley Field, Va., September 26, 1947

REFERENCES

1. Mayo, Wilbur L.: Analysis and Modification of Theory for Impact of Seaplanes on Water. NACA TN No. 1008, 1945.

2. Wagner, Herbert: Über Stoss- und Gleitvorgänge an der Oberfläche von Flüssigkeiten. Z.f.a.M.M., Bd. 12, Heft 4, Aug. 1932, pp. 193-215.

3. Milwitzky, Benjamin: A Theoretical Investigation of Hydrodynamic Impact Loads on Scalloped-Bottom Seaplanes and Comparisons with Experiment. NACA TN No. 1363, 1947.

4. Pabst, Wilhelm: Theory of the Landing Impact of Seaplanes. NACA TM No. 580, 1930.

5. Miller, Robert W., and Leshnover, Samuel: Hydrodynamic Impact Loads in Smooth Water for a Prismatic Float Having an Angle of Dead Rise of 30°. NACA TN No. 1325, 1947.

6. Mayo, Wilber L.: Theoretical and Experimental Dynamic Loads for a Prismatic Float Having an Angle of Dead Rise of $22\frac{1}{2}^\circ$. NACA RB No. L5F15, 1945.

7. Batterson, Sidney A.: The NACA Impact Basin and Water Landing Tests of a Float Model at Various Velocities and Weights. NACA Rep. No. 795, 1944.

8. Batterson, Sidney A.: Variation of Hydrodynamic Impact Loads with Flight-Path Angle for a Prismatic Float at 12° Trim and with a $22\frac{1}{2}^\circ$ Angle of Dead Rise. NACA RB No. L5K21a, 1946.

9. Batterson, Sidney A.: Variation of Hydrodynamic Impact Loads with Flight-Path Angle for a Prismatic Float at 3° Trim and with a $22\frac{1}{2}^\circ$ Angle of Dead Rise. NACA RB No. L5A24, 1945.

10. Batterson, Sidney A., and Stewart, Thelma: Variation of Hydrodynamic Impact Loads with Flight-Path Angle for a Prismatic Float at 6° and 9° Trim and a $22\frac{1}{2}^\circ$ Angle of Dead Rise. NACA RB No. L5K21, 1946.

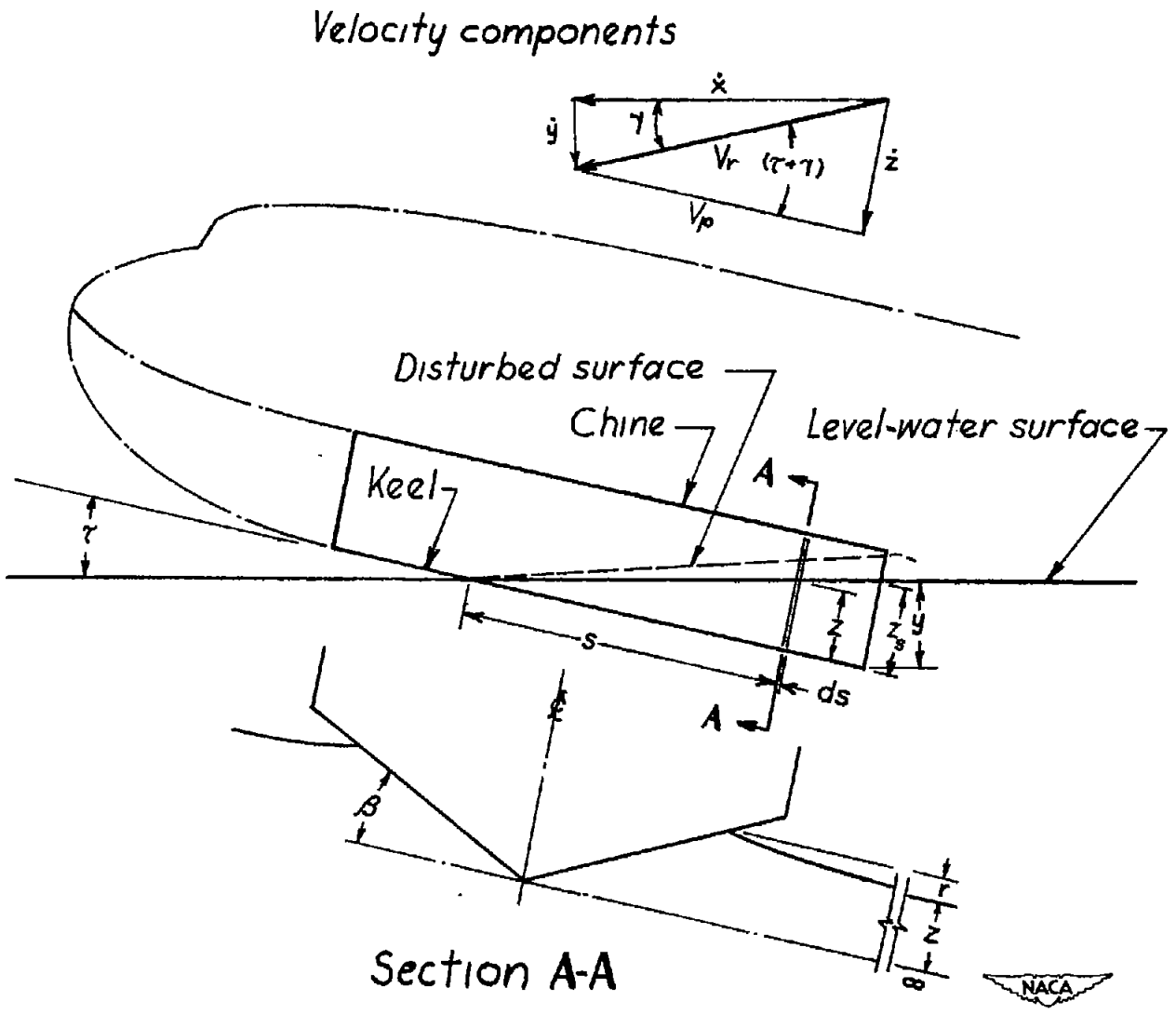

Figure 1.- Schematic representation of impact.

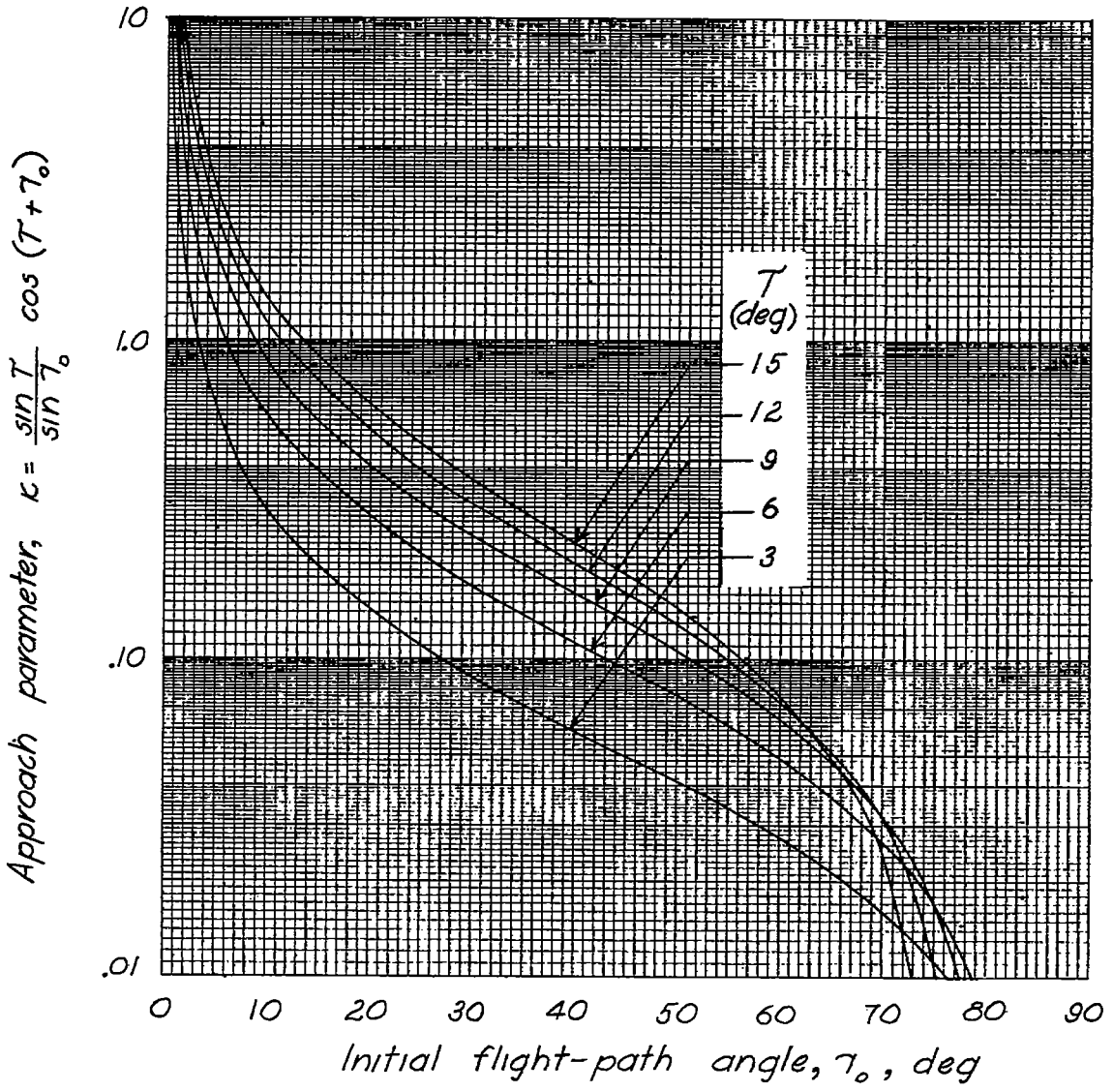

Figure 2. — Variation of approach parameter with trim and flight-path angle.

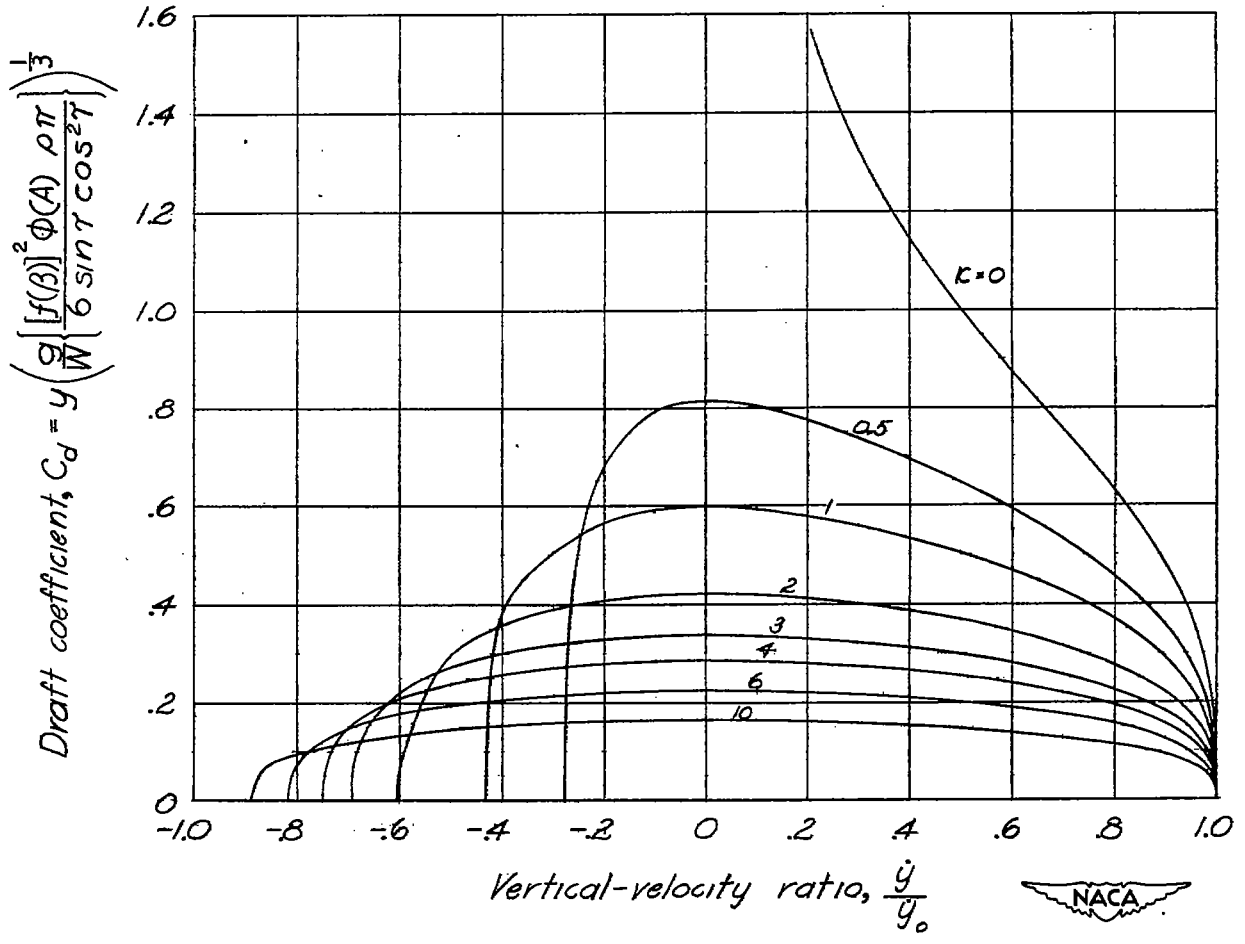

Figure 3. — Theoretical variation of draft with vertical velocity. Approach parameter $\kappa = \frac{\sin\gamma}{\sin\gamma_0}\cos(\gamma+\gamma_0)$.

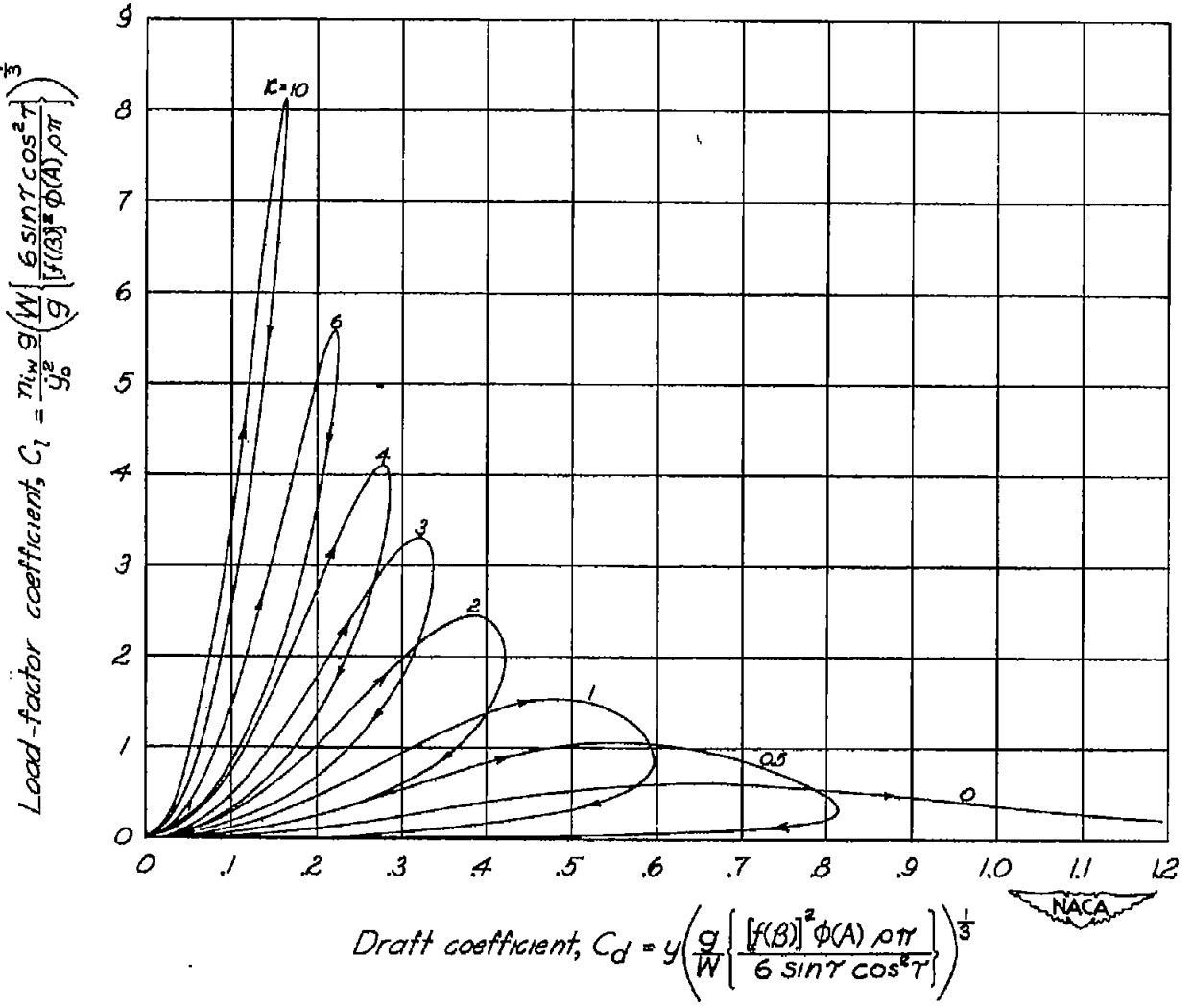

Figure 4. —Theoretical variation of load factor with draft. Approach parameter $K = \frac{\sin\gamma}{\sin\gamma_o} \cos(\gamma+\gamma_o)$.

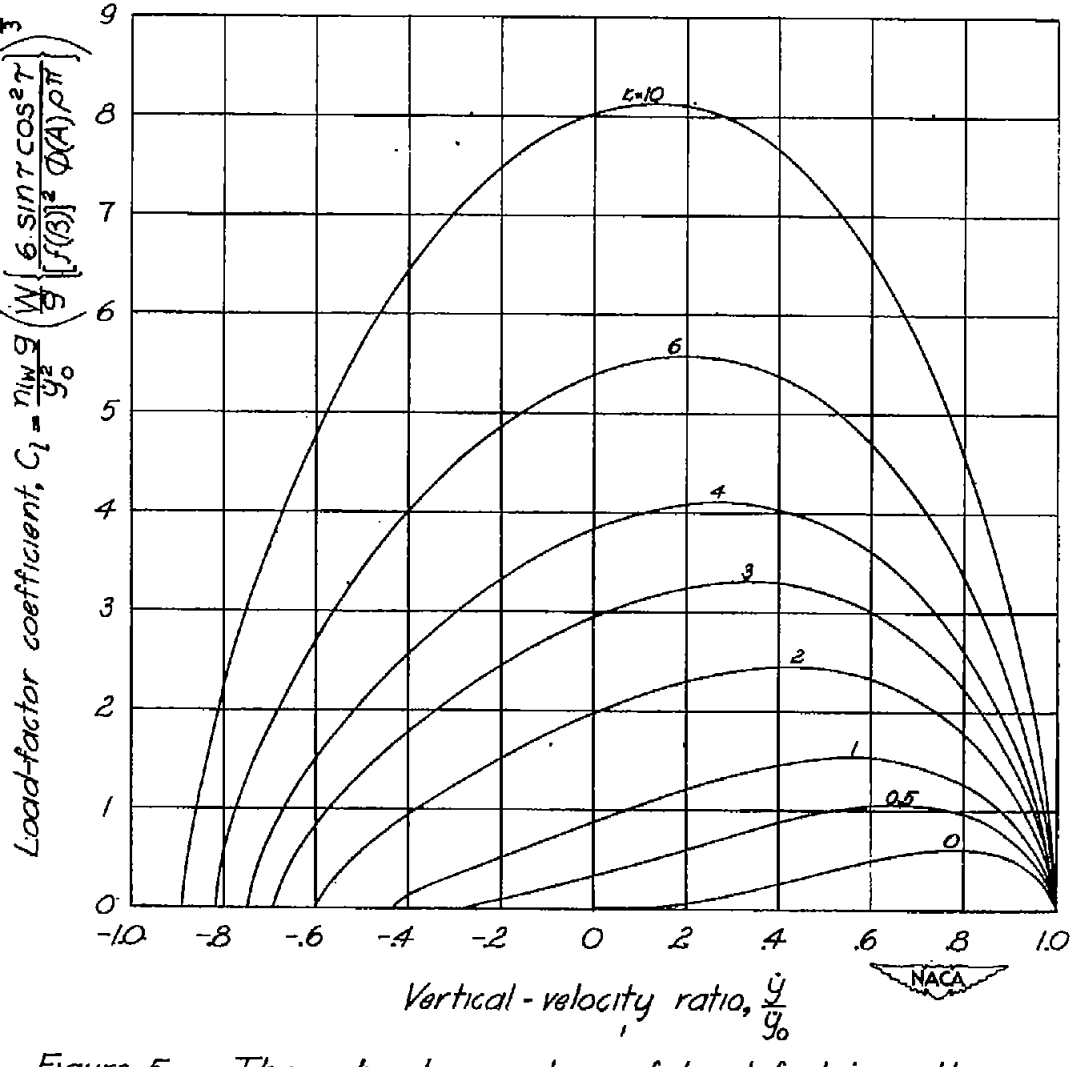

Figure 5.— Theoretical variation of load factor with vertical velocity. Approach parameter $\kappa = \frac{\sin\tau}{\sin\gamma_o}\cos(\tau+\gamma_o)$.

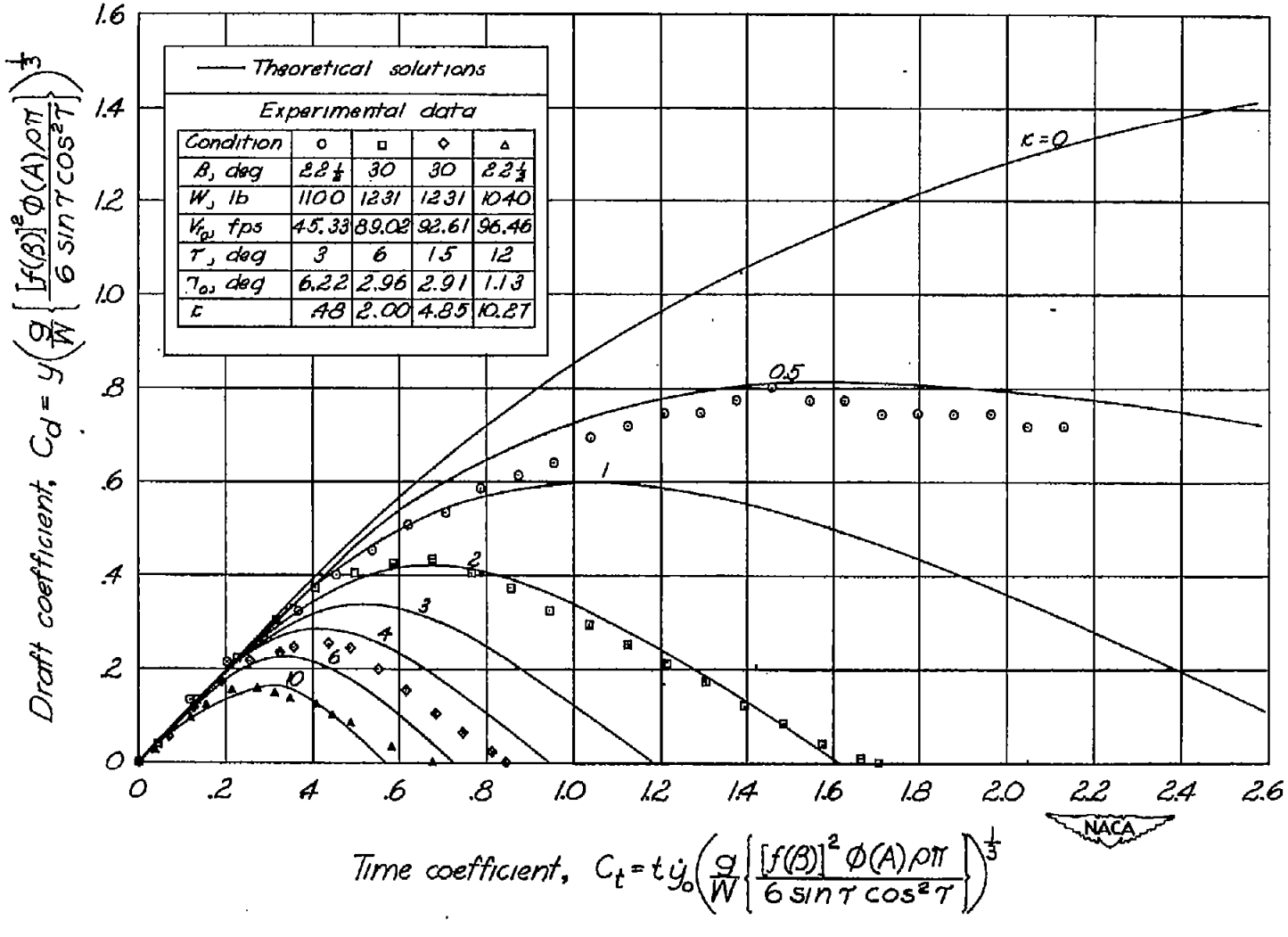

Figure 6.— Comparison between theoretical and experimental time histories of draft. Approach parameter $\kappa = \frac{\sin\tau}{\sin\gamma_0}\cos(\tau+\gamma_0)$.

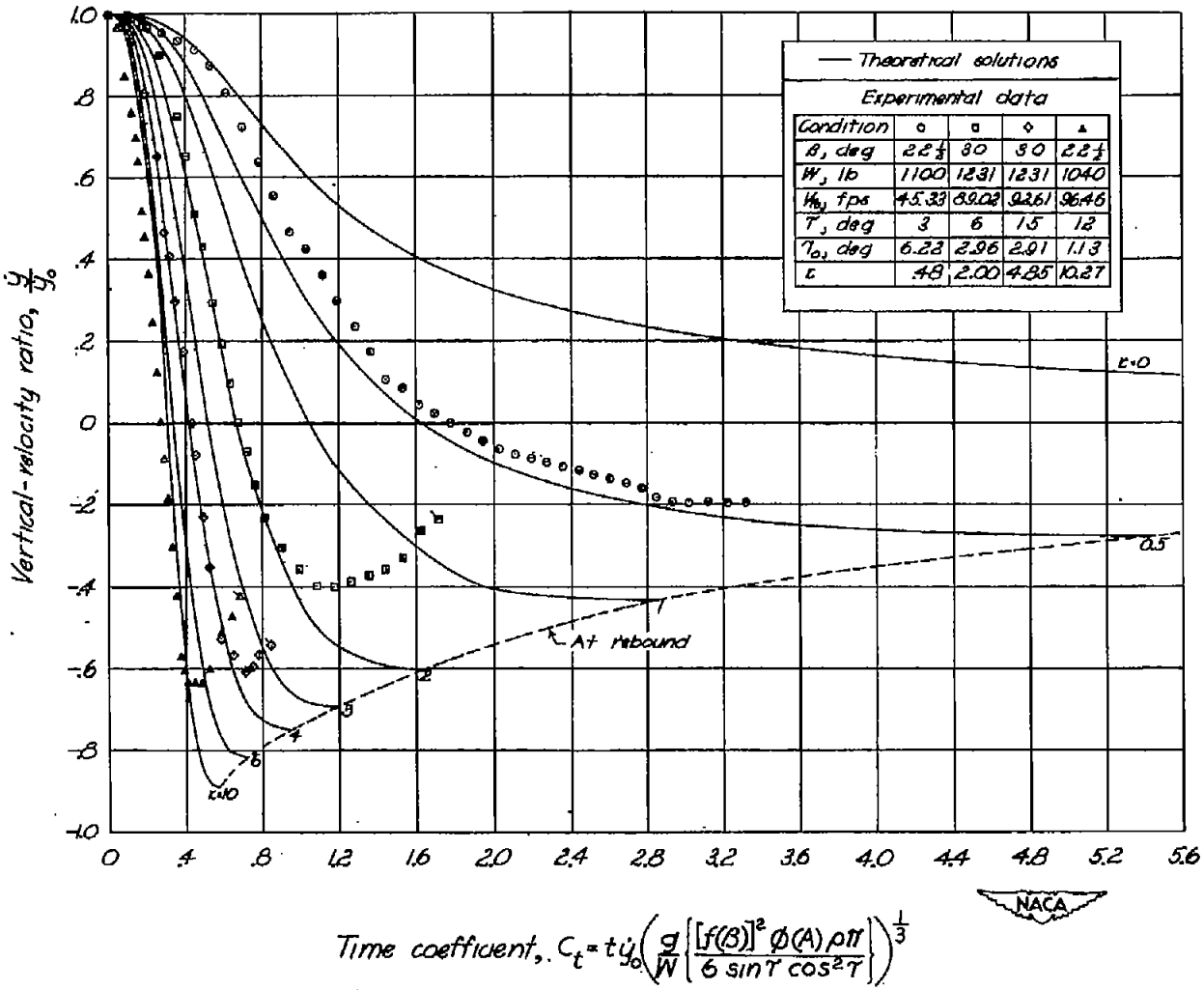

Figure 7. — Comparison between theoretical and experimental time histories of vertical velocity. Approach parameter $\kappa = \frac{\sin\gamma}{\sin\gamma_0}\cos(\gamma+\gamma_0)$.

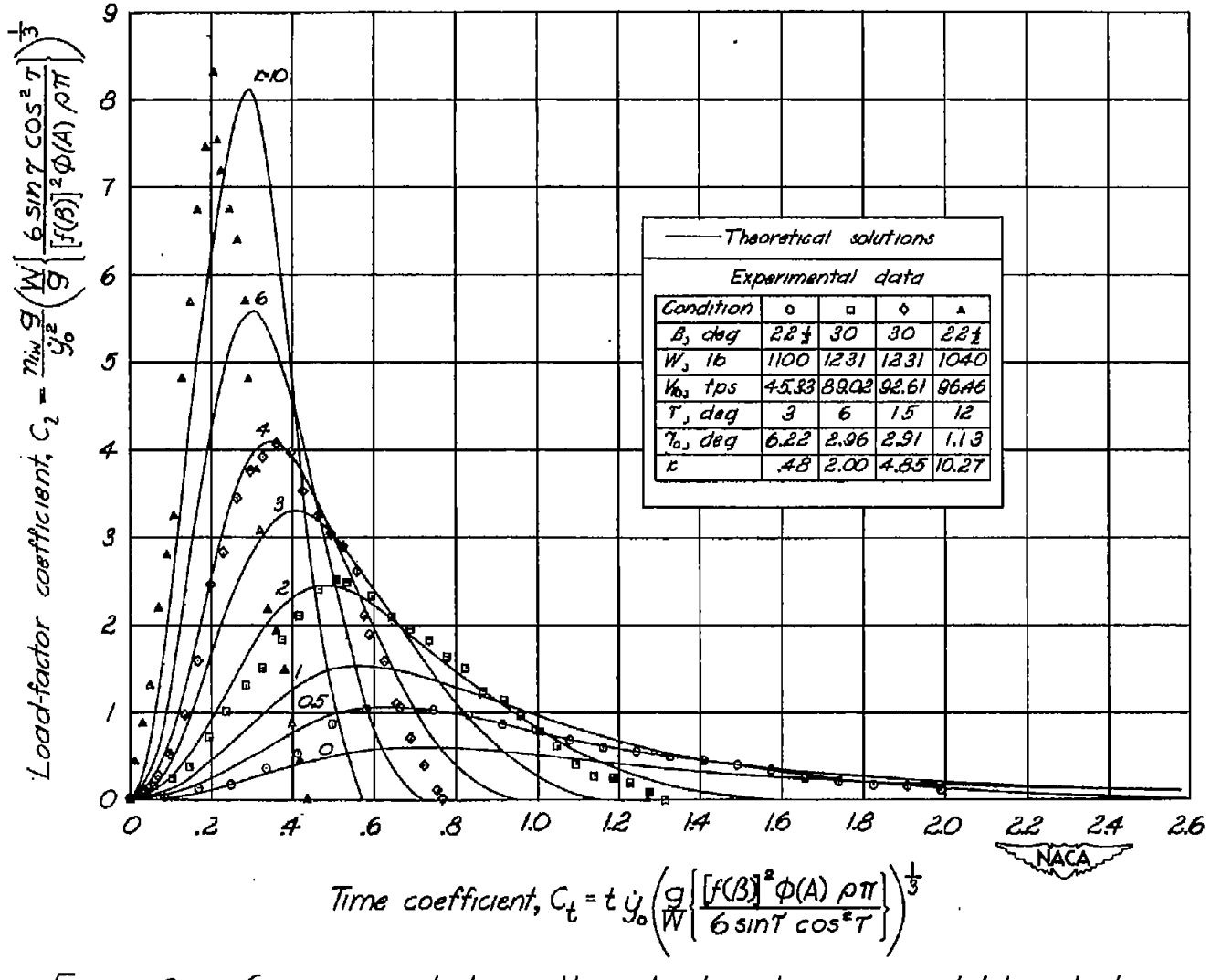

Condition	○	□	◇	△
β_1, deg	22½	30	30	22½
W_1, lb	1100	1231	1231	1040
V_{0_1}, fps	45.33	89.02	92.61	96.46
τ_1, deg	3	6	15	12
τ_{0_1}, deg	6.22	2.96	2.91	1.13
κ	.48	2.00	4.85	10.27

Figure 8.— Comparison between theoretical and experimental time histories of load factor. Approach parameter $\kappa = \frac{\sin\tau}{\sin\tau_o}\cos(\tau+\tau_o)$.

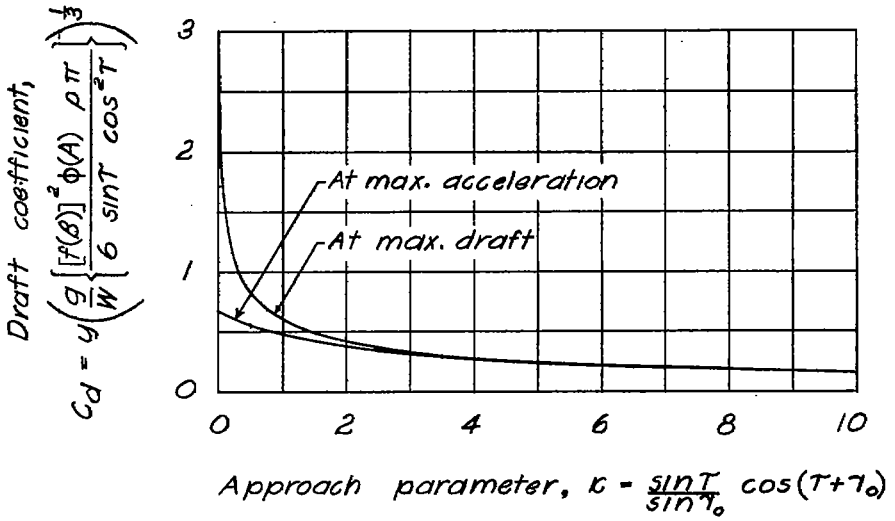

(a) Draft coefficient.

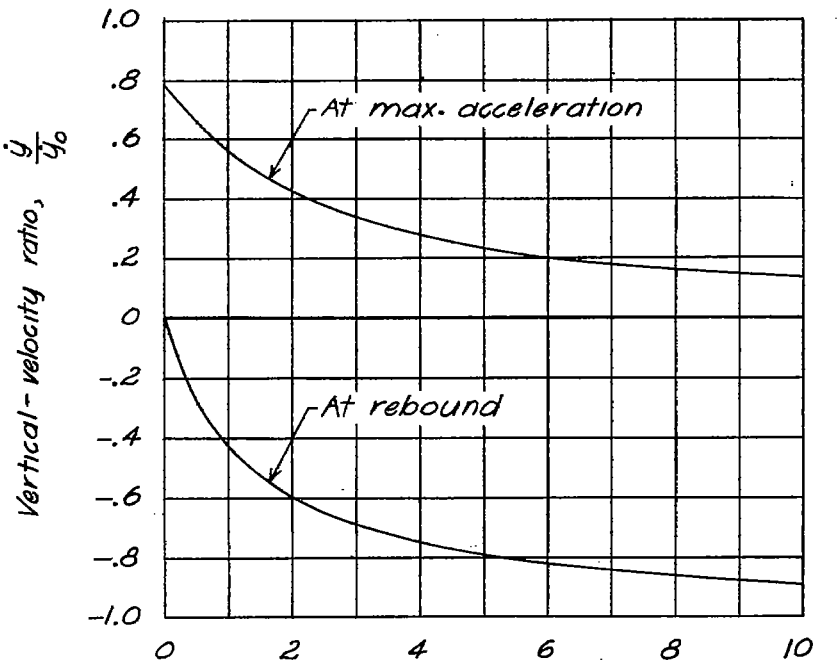

(b) Vertical-velocity ratio.

NACA

Figure 9. — Theoretical variation of the motion variables with approach parameter.

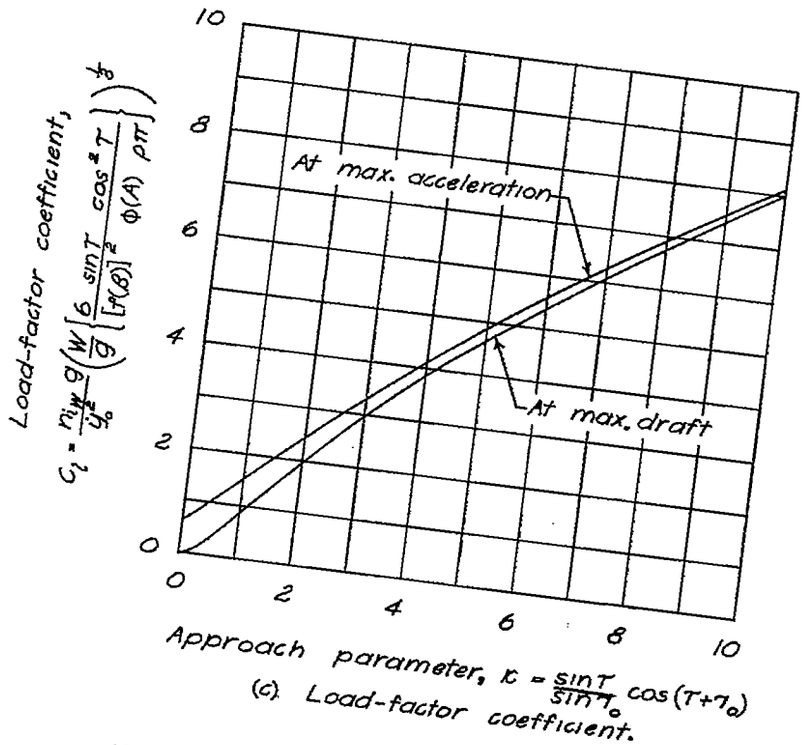

(c) Load-factor coefficient.

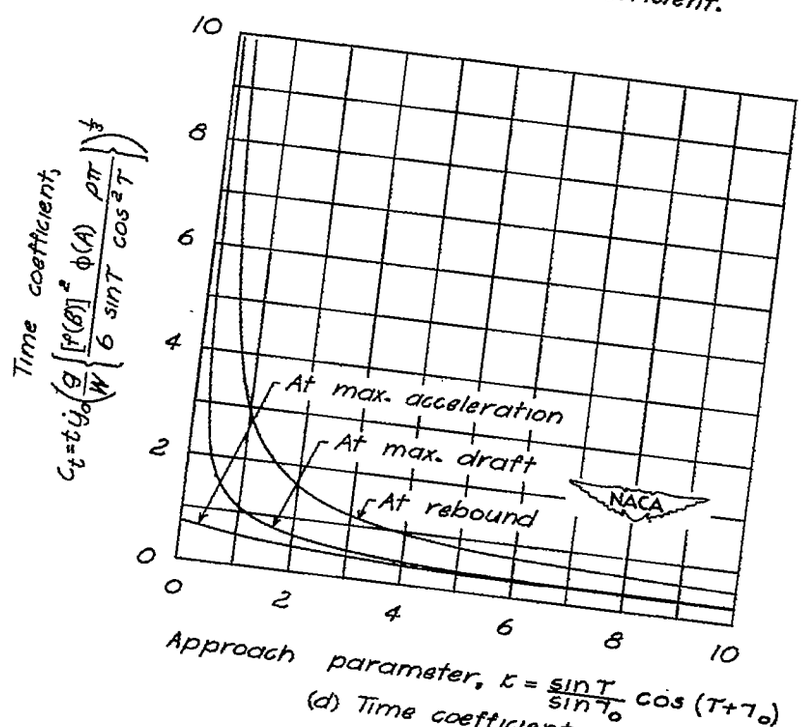

(d) Time coefficient.

Figure 9. — Concluded.

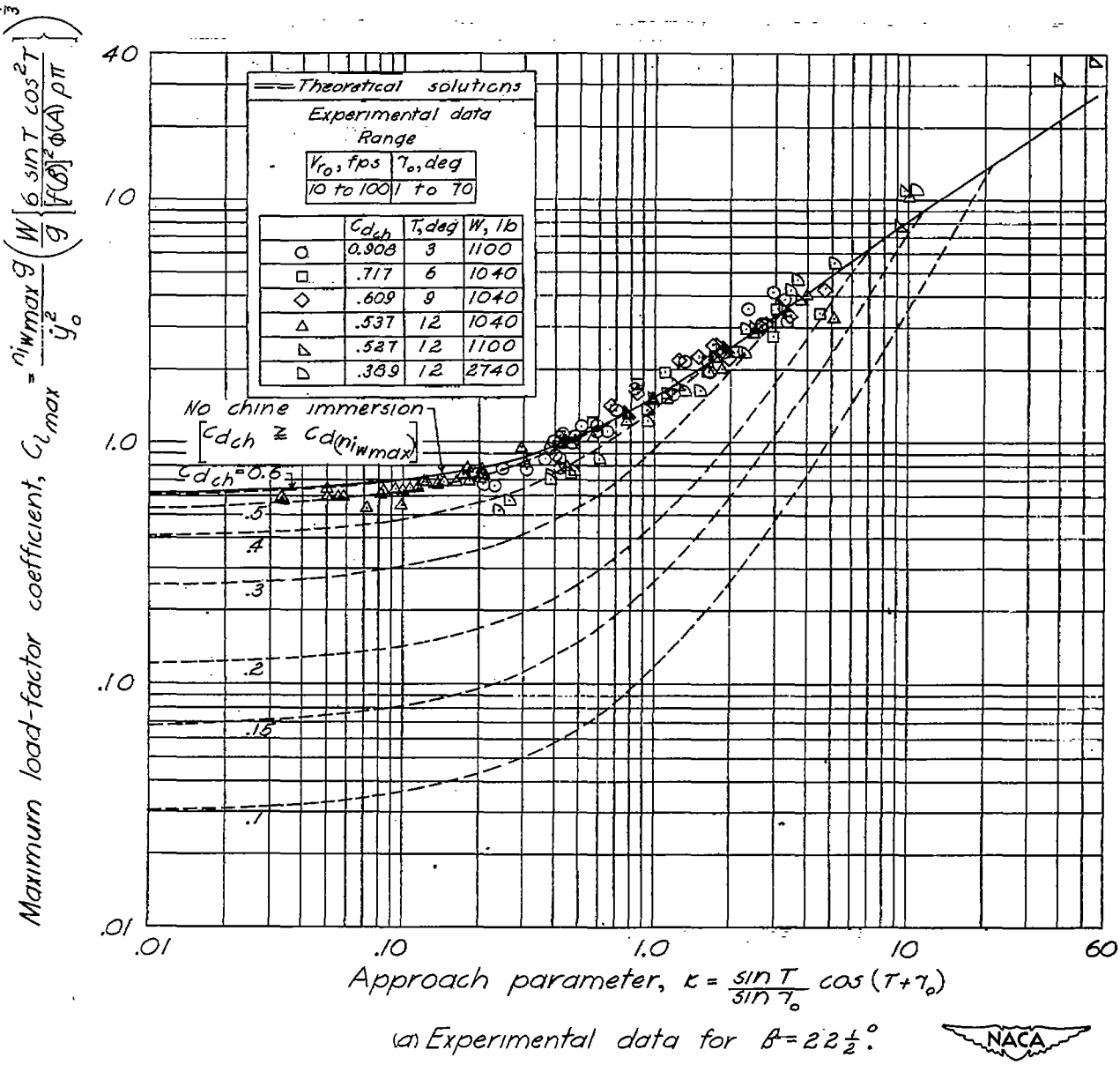

Figure 10.— Comparison of theoretical and experimental variation of maximum load-factor coefficient with κ, including the effects of chine immersion.

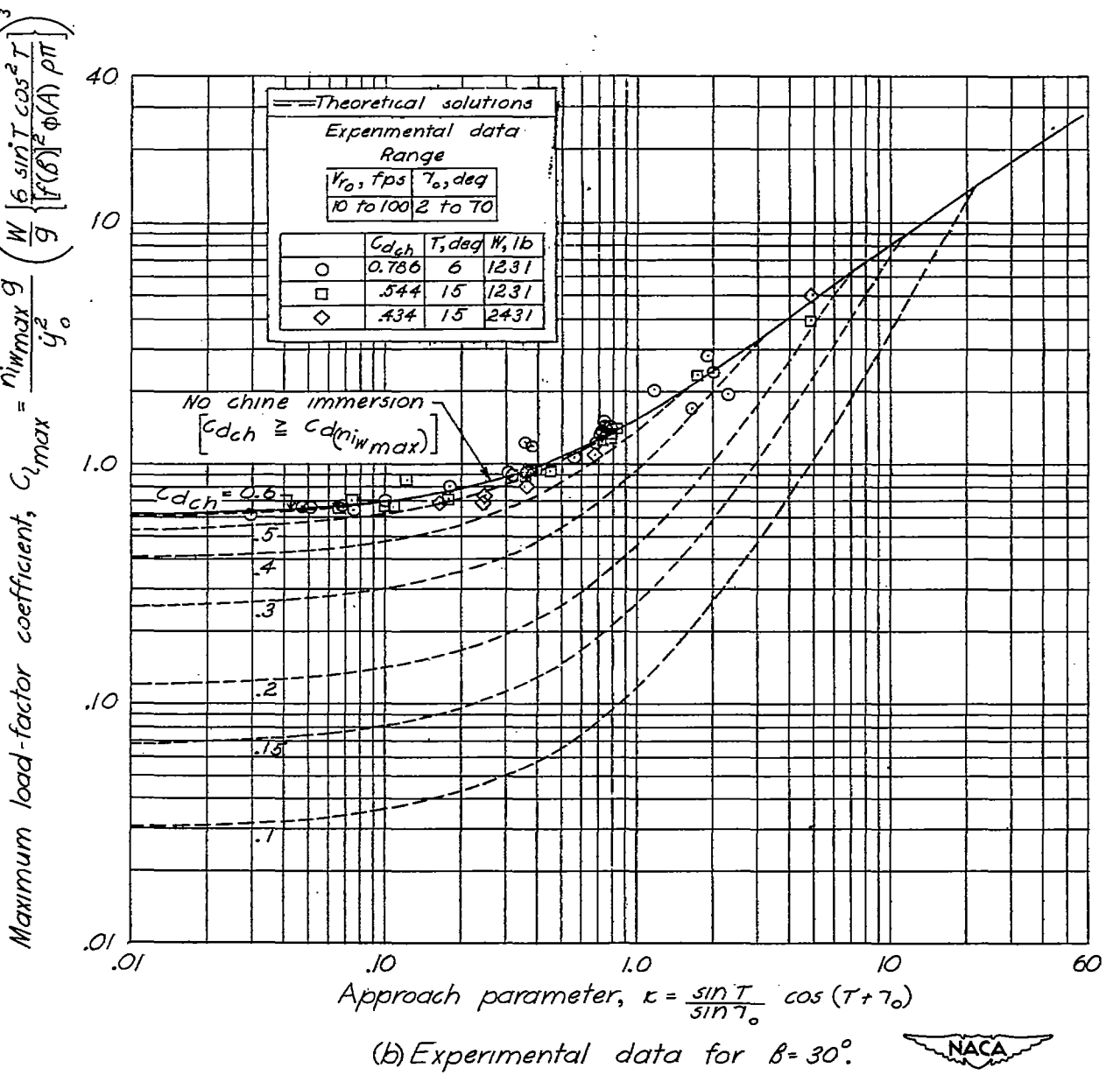

(b) Experimental data for $\beta = 30°$.

Figure 10. —— Continued.

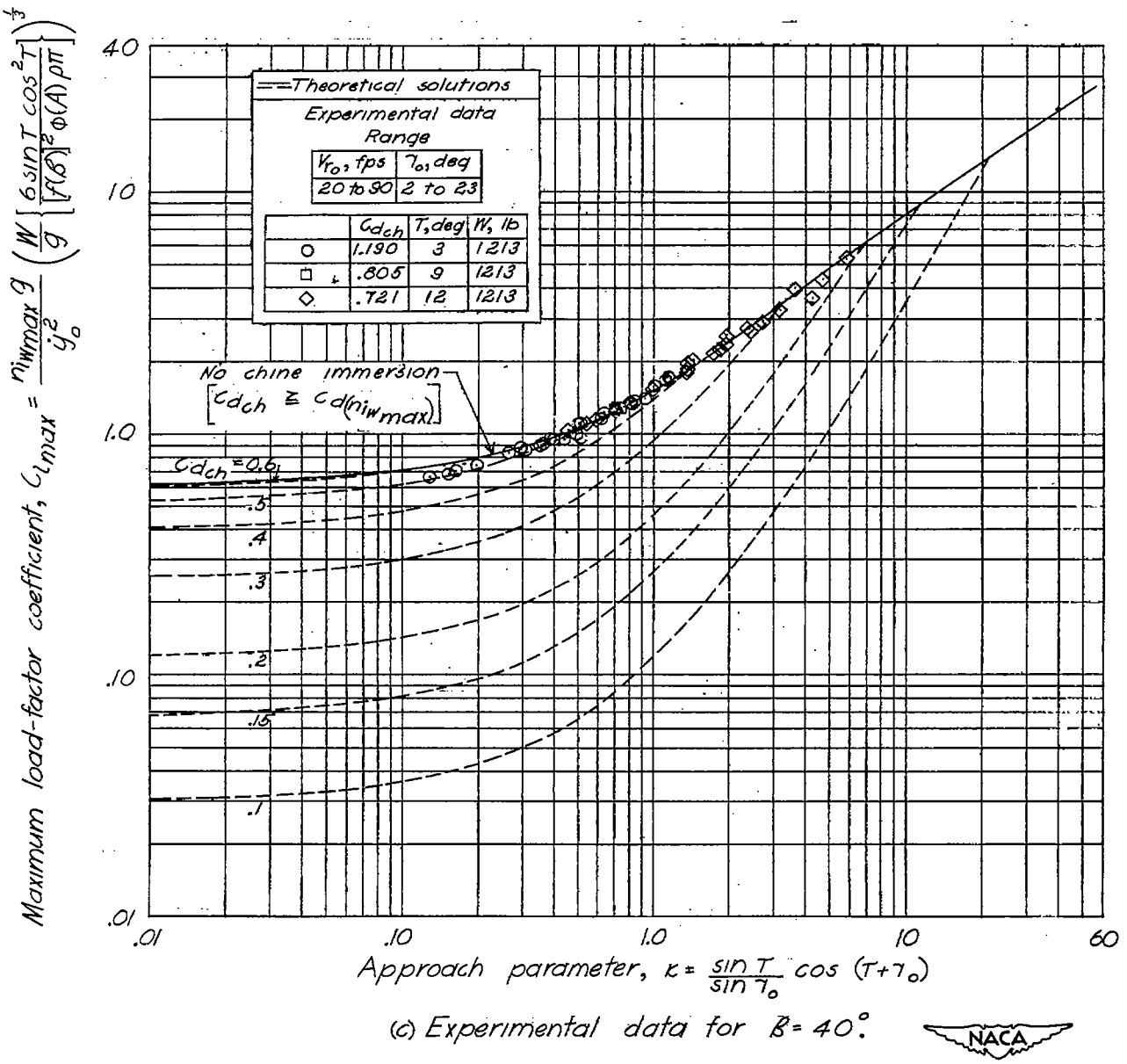

(c) Experimental data for $\beta = 40°$.

Figure 10. — Concluded.

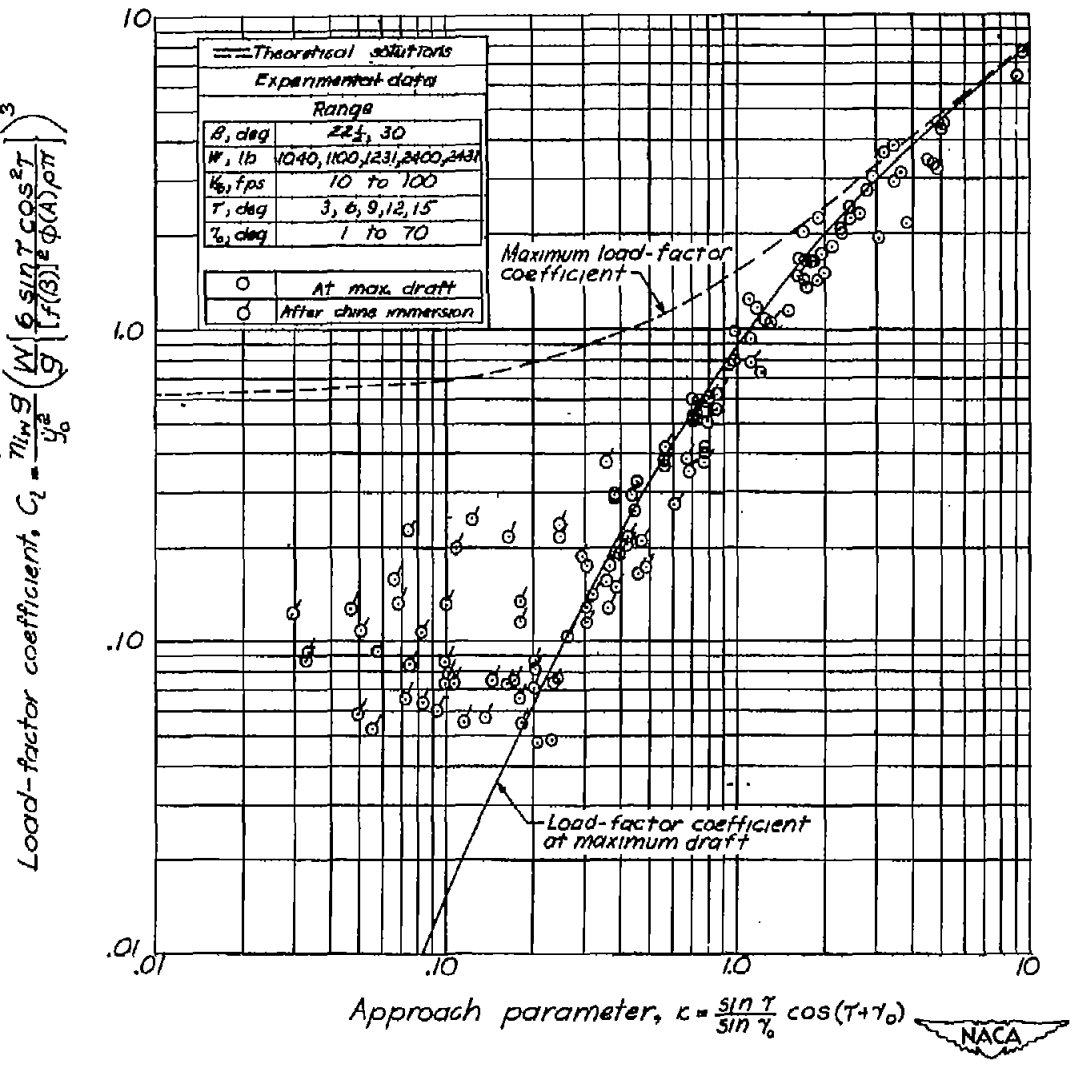

Figure 11.— Comparison between theoretical and experimental variation of load factor at maximum draft with approach parameter.

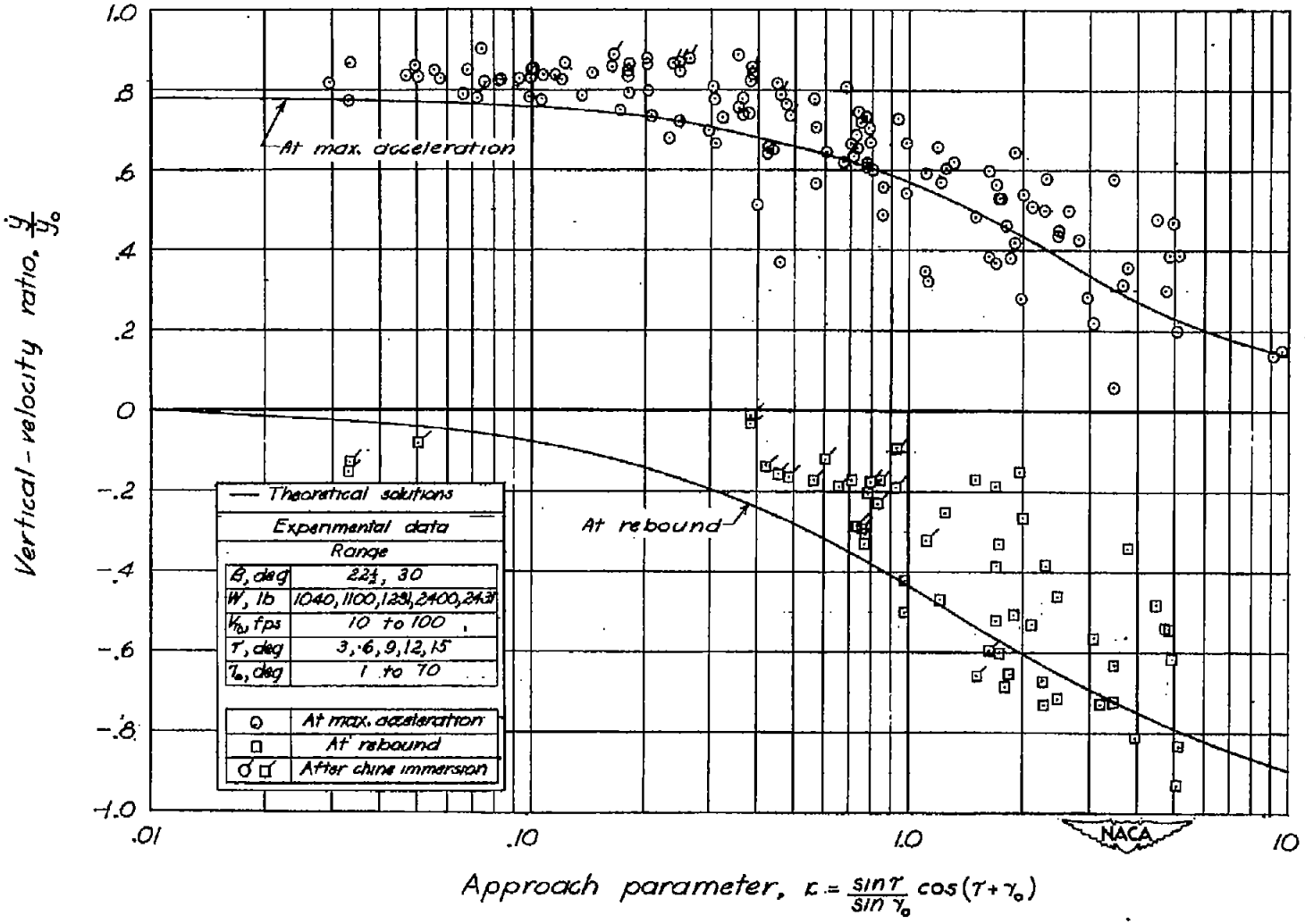

Figure 12. — Comparison between theoretical and experimental variation of vertical velocity with approach parameter.

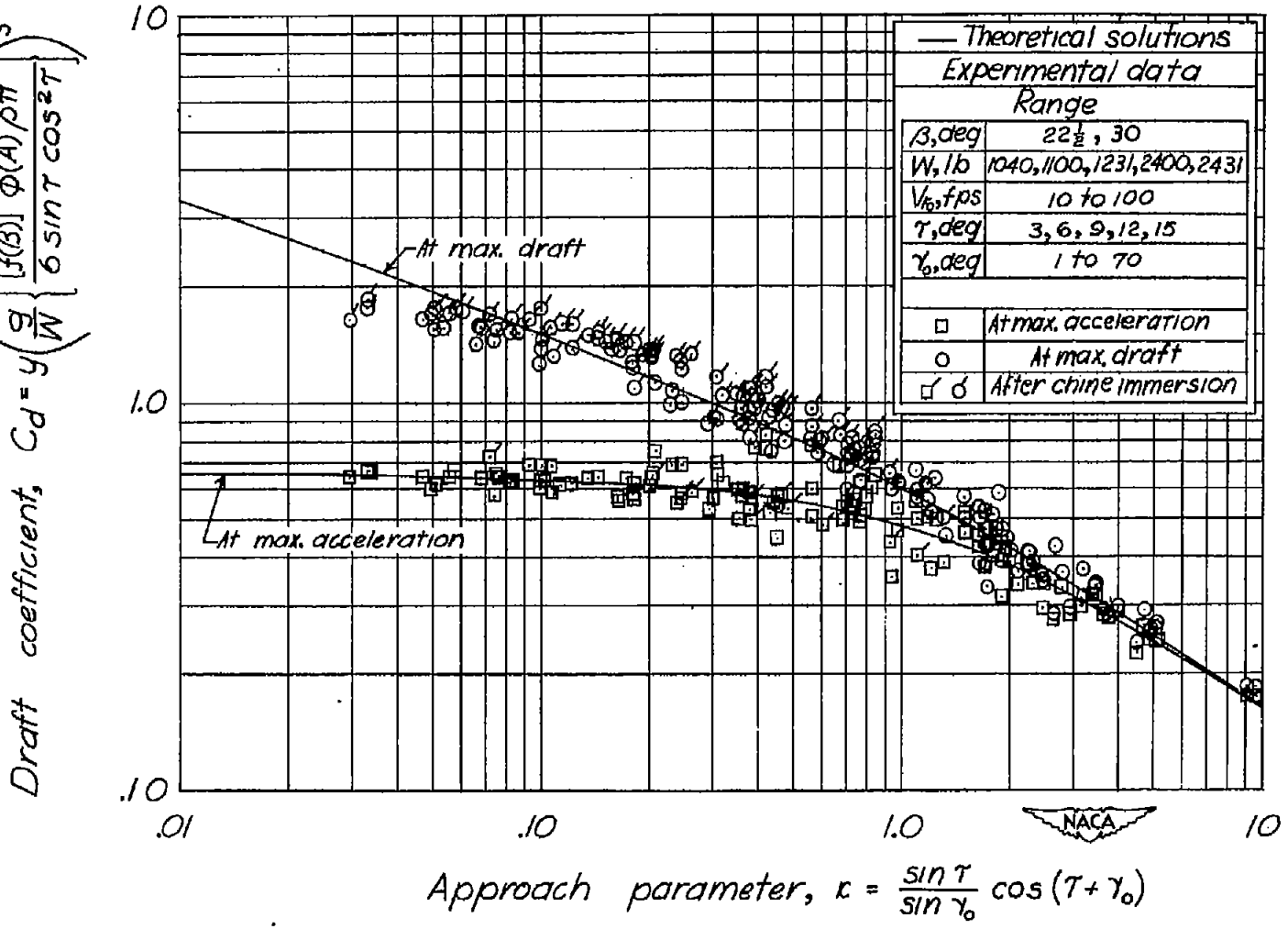

Figure 13.— Comparison between theoretical and experimental variation of draft with approach parameter.

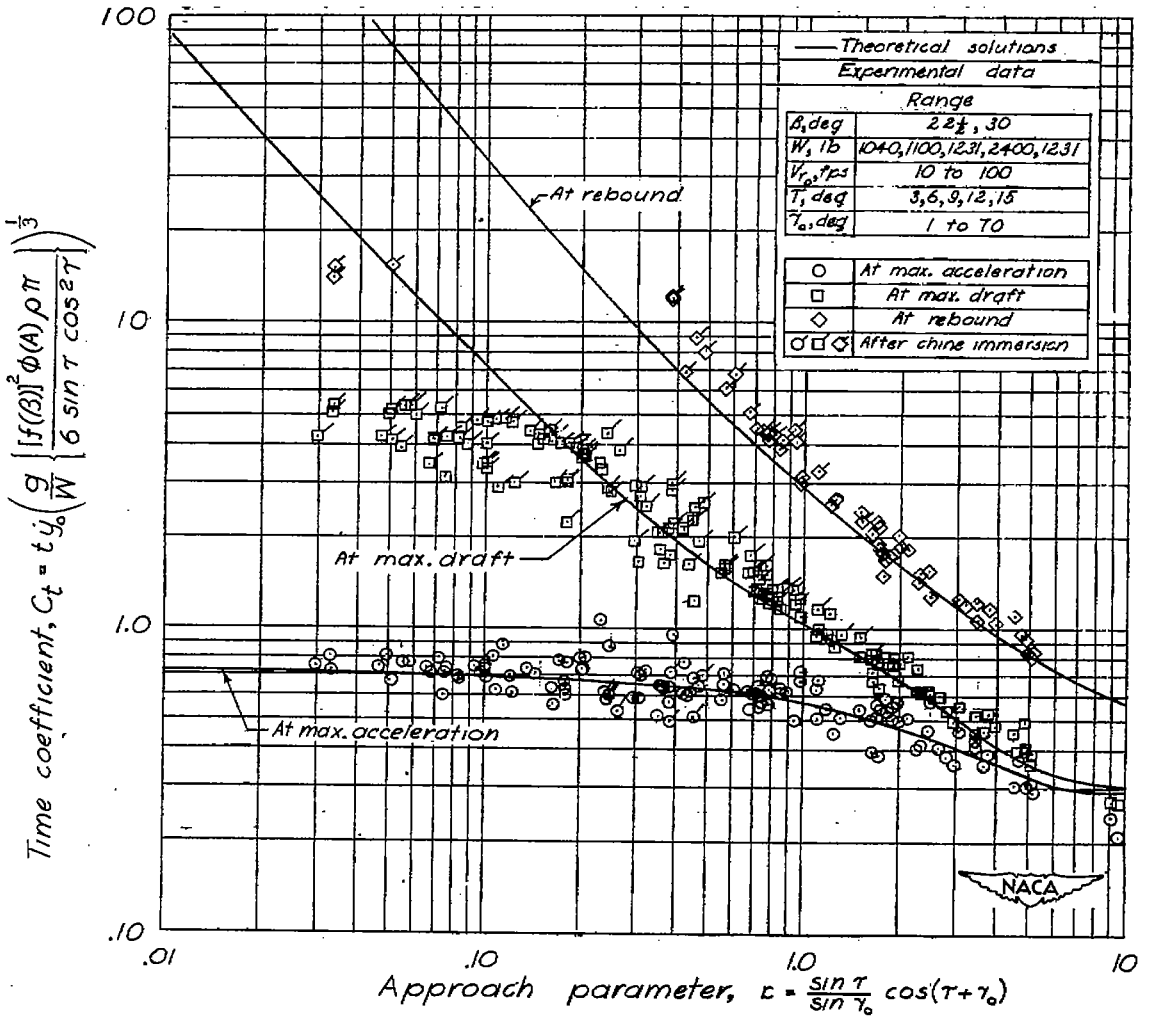

Figure 14. — Comparison between theoretical and experimental variation of time with approach parameter.